CMLS, Cell. Mol. Life Sci. 56 (1999) 604–625
1420-682X/99/080604-22 $ 1.50 + 0.20/0

CMLS Cellular and Molecular Life Sciences

Review

Nickel-binding proteins

R. K. Watt† and P. W. Ludden*

433 Babcock Dr., Madison (Wisconsin 53706, USA), Fax + 1 608 262 3453, e-mail: Ludden@biochem.wisc.edu

Received 25 February 1999; received after revision 5 July 1999; accepted 8 July 1999

Abstract. Nickel enzymes are a relatively new class of metalloenzymes. The seven known nickel enzymes are urease, hydrogenase, CO-dehydrogenase, methyl-coenzyme M reductase, Ni-superoxide dismutase, glyoxalase I and cis-trans isomerase. The requirement for nickel implies the presence of a nickel-processing system, since free transition metals are harmful to the cell. A nickel-processing system involves the recognition and transport of nickel into the cell and the handling of the nickel once it enters the cell until it is inserted into the nickel enzyme. Several mechanisms for nickel transport have been identified and will be reviewed here. Accessory proteins required for the biosynthesis of the nickel active site have been identified. Accessory proteins bind the nickel when it enters the cell and are proposed to assist with the insertion of nickel into the enzyme. The function of the characterized nickel-processing proteins is described, and models for nickel insertion into the nickel enzymes are presented.

Key words. Nickel enzymes; nickel transport; nickel-processing proteins; metal chaperonin proteins; metallocluster assembly; urease; hydrogenase; CO-dehydrogenase.

Introduction

Nature has harnessed the rich and varied chemistry of the transition metals to catalyze a variety of biological reactions essential to sustain life. The reactivity of the transition metals depends on the ligands, coordination geometry and oxidation state of the metal. Biological systems have taken advantage of the transition metals' reactivity by coordinating the metal(s) in the framework of a protein structure that controls the reactivity and oxidation states of the metal(s). Although the transition metals catalyze life-sustaining metabolic reactions, they also catalyze reactions that are harmful to the cell. Redox reactions catalyzed by metal ions in the cytosol damage proteins, lipids and DNA. Metal ions can bind to enzymes, causing inhibition or inactivation of the enzymatic activity. Transition metals also bind very efficiently to DNA, causing damage to vital genetic material. To avoid harmful side reactions, biological systems have developed mechanisms to transport, escort and insert transition metals into the appropriate metalloenzyme. Metal transport and chaperone systems keep the metal sequestered in such a manner that the metal is 'inert' until the metal is inserted into the active site of the proper enzyme.

The discovery of nickel in the active site of the enzymes urease, hydrogenase, CO-dehydrogenase (CODH), methyl-coenzyme M reductase and the recently discovered Ni-superoxide dismutase and glyoxalase I enzymes has created a very active field exploring the biochemistry of nickel (for reviews see [1–7]). Molecular biology and biochemistry and spectroscopy have been used to identify and characterize nickel transport systems, nickel-binding proteins and chaperonin-like proteins that are required for the insertion of nickel into the nickel enzymes.

† Current address: Princeton University, Department of Chemistry, 17 Hoyt Lab., Princeton (New Jersey 08544, USA), Fax + 1 609 258 1980, e-mail: rwatt@princeton.edu
* Corresponding author.

For the purpose of this review we define nickel-binding proteins as (i) proteins involved in the recognition, binding and transport of nickel into the cell; (ii) proteins involved in binding and sequestering the nickel once it enters the cell; (iii) proteins required for the insertion of nickel into the nickel enzyme; (iv) the nickel enzyme. This review will begin with a brief discussion of the nickel enzymes and the reactions performed by these enzymes. The discussion of the nickel enzymes is not meant as an extensive review of each of the nickel enzymes, because detailed reviews are found elsewhere (see [1–7]). Rather, the discussion of the nickel enzymes provides the biochemical and structural information necessary to understand the requirements for the nickel-binding proteins and chaperonin/insertion proteins that participate in assembling the nickel active sites. After describing the nickel enzymes, discussion will focus on the metabolism of nickel from its transport into the cell until its insertion into the nickel enzyme. The review will conclude by comparing the common requirements among the nickel-processing systems.

Nickel-containing enzymes

Nickel enzymes are a relatively new class of enzymes with only six enzymes currently identified. The nickel active site structures of the characterized nickel enzymes are shown in figure 1. These structures have been determined by X-ray crystallography or proposed from spectroscopic analyses of the enzymes.

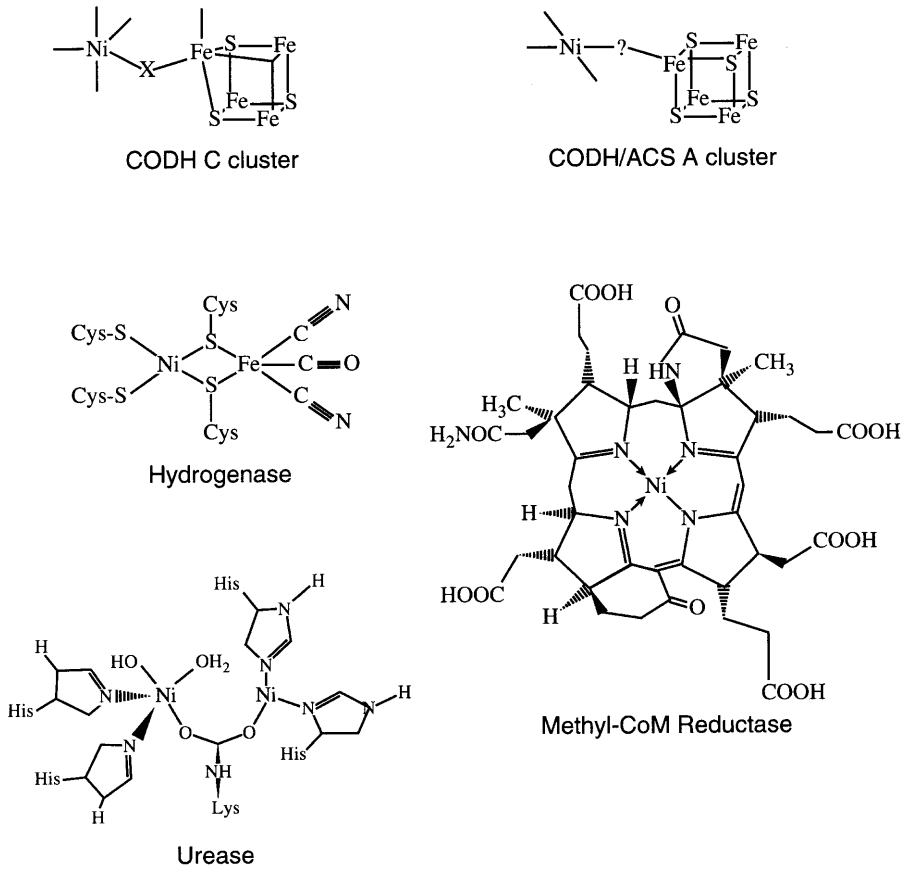

Figure 1. Active sites of Nickel-Containing Enzymes. The proposed active site structures of the C-cluster of CODH and CODH/ACS and the A-cluster of CODH/ACS have been proposed from spectroscopic studies [62, 82]. The structure of the hydrogenase active site has been proposed from X-ray crystallographic studies and infrared studies [35, 41–43]. Recent crystallographic studies show a bridging ligand (O or S) between the Fe atom and the Ni atom in hydrogenase, but the assignment of the ligand is controversial [6, 37]. The structures of the active sites of urease and methyl-CoM reductase were determined by X-ray crystallography [17, 93]. The structure of urease from *Bacillus pasteurii* shows a bridging hydroxide between the Ni atoms and the remaining coordination sites to nickel completed with water [11].

Urease

Urease has the historical distinction of being the first enzyme crystallized [8] and the first demonstrated to contain nickel [9], although 50 years separated the first event from the second. Urease is found in bacteria, fungi and plants, and catalyzes the hydrolysis of urea yielding ammonia and carbamate as shown in equation 1.

$$NH_2CONH_2 + H_2O \leftrightarrow NH_2COOH + NH_3$$

$$\downarrow$$

$$NH_2COOH + H_2O \leftrightarrow NH_3 + H_2CO_3$$

The carbamate product is unstable and spontaneously degrades to ammonia and carbonic acid.

Urea is metabolized by bacteria and plants as a source of nitrogen [10], and this reaction is a source of concern for agricultural and medical reasons. Agriculturally, the efficiency of nitrogen fertilizers applied to the soil for agricultural purposes is severely decreased by urease activity [11]. Medically, the presence of urease activity has been correlated as a virulence factor in several bacteria. The most significant medical problems are the development of urinary stones [12], acute pyelonephritis [13], urinary catheter obstructions [14] and the development of peptic ulcers [15, 16].

The subunit compositions and quaternary structures of urease enzymes from plants and bacteria differ significantly. The plant enzyme is a homohexamer ($\sim$ 550,000 kDa) [9], and the bacterial enzyme is a trimer of trimers [$(\alpha\beta\gamma)_3$]) ($\sim$ 100,000 kDa) [17]. Despite the different quaternary structures and sizes of the enzymes from plants and bacteria, the urease protein sequence contains conserved regions of greater than 50% identity. The difference between the plant and bacterial protein structure appears to result from a gene fusion or disruption of events that occurred during the evolution of the enzyme [18]. The nickel active site appears to have been conserved in plants and bacteria, as two nickel atoms are associated with each active site of the respective enzymes.

The structure of the urease active site has been determined by X-ray crystallography using protein purified from *Klebsiella aerogenes* [17, 19] and *Bacillus pasteurii* [11, 20]. Both structures show a carbamylated lysine residue as a bridging ligand to the two nickel atoms in the active site. The carbamylation is required for catalytic activity as shown by chemical rescue of mutants lacking the lysine residue [21]. The active site is opened and closed by a mobile α-helical flap. The structures differ in the number of nonprotein ligands to the two nickel atoms, and this discrepancy has led to two different proposals for the mechanism of catalysis.

The *K. aerogenes* native enzyme as well as apourease and several active site mutants have also been crystallized and the structures determined [17, 19, 22]. The structures of the *K. aerogenes* urease show a tricoordinate nickel and a pentacoordinate nickel. These data conflict with spectroscopic data indicating the presence of slightly distorted octahedral nickel ions with hexa- or penta-coordination [23]. This structure shows two nickel atoms 3.5 Å apart that are bridged by the carbamylated lysine residue (fig. 1). The proposed catalytic mechanism involves the binding of the oxygen of urea to the tricoordinate nickel atom. His-219 is proposed to stabilize the binding of substrate to the enzyme. The water ion coordinated to the six-coordinate nickel atom is activated by a general base and attacks the substrate urea, forming a tetrahedral intermediate. Ammonia is eliminated with assistance of a general acid, completing the reaction [17]. This model is in conflict with two aspects of the accepted mechanism: first, His-320 is proposed to function as a catalytic base but is located on the wrong side of the active site; and second, there is no base with the appropriate pK_a to deprotonate the water bound to the second nickel atom. The authors have proposed a reverse protonation scheme to rationalize this mechanism [24].

The crystal structure of the *B. pasteurii* urease (2.0 Å resolution) shows the resting state of the active site with the coordination sphere of each nickel atom completed with water molecules and a bridging hydroxide. A fourth water molecule was identified that completed a tetrahedral cluster of water molecules [11]. A structure of urease crystallized in the presence of phenylphosphorodiamidate contains a transition-state analogue, diamidophosphoric acid (DAP), that is bound to the two nickel atoms. A mobile α-helical flap protects the active site and is shown in the 'flap open' configuration in the native structure and 'flap closed' conformation when crystallized with the inhibitor. Benini et al. proposed a mechanism that includes a role for His-323 (equivalent to *K. aerogenes* His-320) and identifies the general base. From the DAP bound to the nickel atoms the authors suggest that the active site binds substrate in an orientation-specific mode and DAP is a transition state analog. Urea is proposed to enter in the 'flap open' conformation and displace the tetrahedral cluster of water molecules. Urea binds to the electropositive 5 coordinate Ni(1) with the carbonyl oxygen, and one of the amino groups binds to Ni(2). The flap closes when urea binds and allows for the carbonyl oxygens of Ala-170 and Ala-366 to hydrogen-bond to the protons of the amino group bound to Ni(2), stabilizing the coordination of nitrogen to Ni. His-323 and His-222 stabilize the transition state. The hydroxide that bridges the two nickel atoms attacks the carbon of urea, causing the hydrolysis. This model is consistent with the spectroscopic data for the coordination sphere of the nickel atoms and uses the biochemical evidence for a general base and His-323.

This mechanism provides rationale for the presence of a bimetallic active site that requires nickel. Although zinc ions are more commonly found in hydrolytic enzymes, nickel is required in urease because nickel has a higher affinity for nitrogen ligands than zinc. The affinity of nickel for nitrogen ligands permits the NH_2 group of urea to bind. Coordination of the nitrogen to nickel permits hydrogen bonds to form with the protons on the amide group, which further stabilizes the binding of the nitrogen to the nickel. Additionally, the bimetallic center with multiple binding sites for water favors nickel over zinc because nickel favors octahedral coordination versus the tetrahedral coordination favored by zinc. The water that bridges the two nickel atoms would be acidic and is proposed to exist in the form of hydroxide (pK_a of Ni bridging hydroxide $\sim 9-10$) that is required for the nucleophilic attack for hydrolysis to occur.

The structure of urease shows two elements of the urease active site that are significant when considering the assembly of the nickel binuclear cluster. The first element is a lysine residue that must be carbamylated to properly coordinate the two nickel atoms. The second element in the active site is buried by a flap that protects the active site. Evidence will be presented later in this review to show that accessory proteins may be involved in the carbamylation of the lysine and that chaperonin-like proteins function to hold the protein open so that nickel can bind to the urease active site.

Hydrogenase

Hydrogenase enzymes catalyze the reversible reaction shown in equation 2.

$$H_2 \leftrightarrow 2H^+ + 2e^- \quad \text{(eq. 2)}$$

The direction of the reaction is used to classify the hydrogenase enzyme. If the in vivo function of the hydrogenase is to consume hydrogen, then the enzyme is classified as an H_2-consuming or uptake hydrogenase. If the enzyme produces H_2, then it is classified as a hydrogen-evolving hydrogenase. Another classification of hydrogenases is made by the metal content and subunit composition of the enzymes. Three classes have been identified: (i) the iron-containing hydrogenase (for review see [25]); (ii) the nickel-iron hydrogenase and the nickel-iron-selenium hydrogenase [26, 27]; and (iii) hydrogenases that contain neither iron nor nickel [28]. The present discussion will focus on the nickel-iron hydrogenases and the incorporation of nickel into the enzyme.

Ni-hydrogenase enzymes with two differing quaternary structures have been identified. One class is composed of two subunits. The large subunit ranges from 45 to 65 kDa and contains the nickel metallocluster active site. There is a high degree of sequence similarity among the large subunits of the NiFe-hydrogenases from various sources, and there is immunological cross-reactivity among the large subunits, indicating that they are structurally similar [29]. The role of the small subunit appears to be in electron transfer from the large subunit, and the small subunits are well conserved but less so than the large subunits [30]. Other nickel-containing hydrogenases are tetramers and are integral membrane proteins [31].

Two motifs have been identified that are involved in the ligation of the nickel. A motif in the N-terminal region is RxCGxC, and a second motif in the C-terminus is DPCxxC. Mutational analysis in hydrogenase 1 of *Escherichia coli* showed that replacement of the conserved amino acids of this protein resulted in complete loss of hydrogenase activity [32]. The role of these motifs in binding nickel was bolstered by comparison to [NiFeSe] hydrogenases. Similar motifs are found in the primary structures with the cysteine in motif 2 replaced by selenocysteine (DPUxxC). The selenocysteine was shown by extended X-ray absorption fine structure (EXAFS) and electron paramagnetic resonance (EPR) to be in close proximity to the nickel in *Desulfovibrio baculatus* [33, 34].

The crystal structure of the 'as purified' (aerobically purified) nickel-iron hydrogenase from *Desulfovibrio gigas* has been solved to 2.85 Å [35]. The hydrogenase from *Desulfovibrio vulgaris* Miyazaki F was purified under strictly anaerobic conditions, and the structure of this protein was determined by X-ray diffraction to 1.8 Å resolution. Very recently, an H_2 reduced form of this hydrogenase was characterized to 1.4 Å resolution. The method of purification affects the active state of hydrogenase because aerobic purification yields an inactive form that can later be activated by reduction of the enzyme [36]. The crystal structures show the active site resides in the 60-kDa large subunit with a Ni atom bridged to a second metal that has been identified as Fe. The Ni and Fe atoms are bridged by two thiolate ligands, and a third bridge is from a monotomic atom which has been suggested to be either oxygen [6, 36] or sulfur [37, 38]. The small subunit (26 kDa) contains two Fe_4S_4 clusters and one Fe_3S_4 cluster. The linear arrangement of the iron-sulfur clusters was proposed to channel electrons away from the active site. The nickel site is deep inside the protein, and in order to place the nickel atom deep within the protein, scaffold proteins may be required to hold the large subunit open. Alternatively, the hydrolysis of a nucleotide triphosphate is proposed to open up the protein to insert the nickel into the active site [39, 40].

The structure of the active site of the nickel hydrogenase (fig. 1) was further defined by studying the infrared spectral region of the *Chromatium vinosum* hydrogenase [41, 42]. This work was essential for determining that iron was the metal bridged to nickel and that the iron

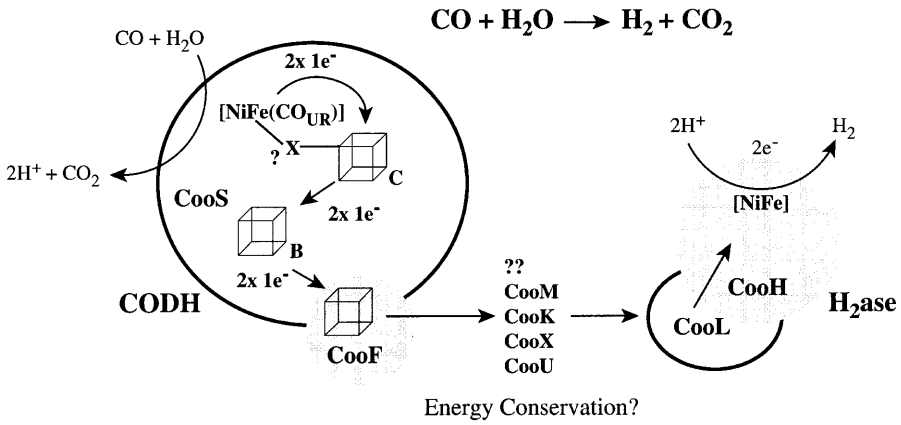

Figure 2. The CO oxidation system of *R. rubrum*. CODH oxidizes CO at the active site, C-cluster. The electrons are passed through the B-cluster to the CooF protein. The electrons then pass through an unknown path proposed to conserve energy. This path may involve the CooM, CooK, CooX and CooU proteins. The electrons are passed to the CO-tolerant hydrogenase (CooL and CooH) where H_2 is produced. The CooC, CooT and CooJ proteins are proposed to insert Ni^{2+} into CODH. This figure was modified from Ludden et al. [192].

atom was coordinated by two CN^- molecules and a CO molecule [43, 44]. The presence of the three diatomic, nonexchangeable ligands as well as an atom bridging the Fe and Ni atoms was observed in a 2.54-Å structure, by isotopic labeling using ^{15}N and ^{13}C, and by chemical analysis [36, 44]. Similar ligands have been detected in Fe-only hydrogenases [45, 46]. The active-site iron was definitively confirmed by comparing difference maps of data collected on both sides of the Fe absorption edge using X-rays from a synchrotron source tuned near the Fe absorption edge [36]. This was also confirmed for the Fe and Ni atoms in *D. vulgaris* Miyazaki F hydrogenase [38]. Furthermore, studies with the *D. vulgaris* Miyazaki F hydrogenase showed (i) the unusual ligands bound to the Fe atom are CO, CN^- and SO [37]; (ii) a Mg atom is bound 13 Å from the NiFe active site [37]; and (iii) reduction of the enzyme with H_2 releases H_2S, and the structure of the H_2-reduced enzyme no longer has the inorganic sulfur bridge [38]. The presence of SO as a ligand to Fe is currently disputed by several groups [6, 44].

Proposals for the mechanism of hydrogenase have been made from analysis of the structural data [7]. The Ni atom is 5 coordinate with square pyramidal geometry, and the Fe atom is 6 coordinate with distorted octahedral symmetry. No EPR signal is observed for the Fe atom, suggesting a low-spin Fe^{2+} state that is consistent with the proposed ligation of CN^- and CO ligands [7] and Mössbauer data [47]. It is proposed that the redox state of Ni does not change during catalysis [7]. Infrared studies of the high-frequency ligands shifted in different redox states, indicating redox state changes in the Fe atom [36]. Gas accessibility studies have shown a channel that leads directly to the vacant coordination site [6]. These data can be used to propose a model where H_2 binds to a vacant site on the Ni atom. Base-assisted heterolytic cleavage of H_2 occurs with binding of hydride to the Ni atom, with no formal redox change. Electrons are then shuttled through the Fe atom, returning the enzyme to the starting state.

Rhodospirillum rubrum CO-dehydrogenase

When *R. rubrum* is exposed to CO, a metabolic system is induced that oxidizes CO to CO_2 by the reaction shown in equation 3. A model of the CO-oxidation system of *R. rubrum* is shown in figure 1. This system is composed of two enzymes: a CO dehydrogenase that performs the half reaction (eq. 4) and a nickel-containing CO-tolerant hydrogenase that uses the electrons liberated in the first half of the reaction to reduce protons to hydrogen gas (eq. 5).

$$CO + H_2O \leftrightarrow CO_2 + H_2 \quad \text{(eq. 3)}$$

$$CO + H_2O \leftrightarrow CO_2 + 2H^+ + 2e^- \quad \text{(eq. 4)}$$

$$2H^+ + 2e^- \leftrightarrow H_2(g) \quad \text{(eq. 5)}$$

The ability of photosynthetic anaerobic bacteria (*Rhodospeudomonas* spp.) to tolerate CO was first noted by Hirsch [48], whereas Uffen observed CO utilization for growth in *Rhodospeudomonas gelatinosa* [49] and *R. rubrum* [50]. The stoichiometric production of H_2 with CO oxidation indicated the presence of a CO-tolerant hydrogenase functioning in the CO oxidation system [49, 51].

The CO-oxidation system from *R. rubrum* has been characterized, and several of the individual components have been purified and characterized. A model of the *R. rubrum* CO-oxidation system is shown in figure 2.

The CODH from *R. rubrum* has been purified and characterized [52, 53]. CODH was shown to be a heat-stabile and O_2-labile 66.9-kDa monomer that contains one Ni atom and eight to nine iron atoms. Data from ultraviolet/visible and EPR spectroscopies are consistent with the iron atoms being arranged in two Fe_4S_4 clusters [53].

When *R. rubrum* is grown on CO in nickel-depleted medium, the CODH protein accumulates in an inactive, nickel-deficient form in the cell [54]. The addition of 2 μM $NiCl_2$ to the medium caused the activity of CODH and hydrogenase to increase several hundredfold, indicating that in vivo activation of both of these enzymes is dependent on nickel [54]. Nickel-deficient CODH (apo-CODH) was purified and contained 0–0.2 Ni atoms per monomer and eight to nine iron atoms per monomer. The addition of nickel and reductant to purified apo-CODH activated the enzyme to specific activities similar to CODH purified from cells grown on nickel [54, 55]. Nickel was the only divalent metal able to activate apo-CODH [54], whereas Cd^{2+}, Zn^{2+}, Co^{2+} and Fe^{2+} all competitively inhibited activation of apo-CODH by Ni^{2+} [55]. In fact, the competing divalent metals all bound to CODH with greater affinity than Ni^{2+} [55].

Ensign showed that nickel was required for the transfer of electrons from CO to the Fe_4S_4 clusters in CODH [56]. The Fe_4S_4 clusters of apo-CODH were not reduced when the enzyme was incubated with CO. When nickel-containing (holo) CODH was incubated with CO, the Fe_4S_4 clusters were rapidly reduced. Cobalt-substituted CODH was the only metal-substituted form of CODH that allowed transfer of electrons from CO to the Fe_4S_4 clusters, and this transfer occurred at a much slower rate. Recently an altered form of CODH in which His-265 replaces valine, H265V, has been characterized and has a 1000-fold lower enzyme activity than wild-type CODH. Both Ni-containing and Co-containing H265V CODH exhibit low activity [57]. These results indicated that nickel or an appropriate analog is required to mediate the transfer of electrons from CO to the Fe_4S_4 clusters.

CODH has been extensively characterized by inhibitors and spectroscopic methods, but this work will not be reviewed here [54–56, 58–63].

CODH/acetyl-CoA synthase

The CO-dehydrogenases from acetogenic and methanogenic bacteria are bifunctional enzymes that perform the reversible CO-oxidation reaction and also function to synthesize or degrade acetyl-coenzyme A (CoA) [64]. The bifunctional characteristics of this enzyme lead to changing the name of the enzyme to CO-dehydrogenase/acetyl-CoA synthase (CODH/ACS) [64]. Both catalytic sites for the individual reactions require nickel for catalysis. However, the active sites of the two enzymatic activities are at different sites [65]. The properties of the enzymes studied from acetogenic and methanogenic bacteria are reviewed below.

Acetogenic bacteria are anaerobes that produce acetate as a product of autotrophic growth on CO_2 and H_2 or as a product of sugar fermentation. CO_2 is reduced to CO for use in the Wood-Ljungdahl pathway for autotrophic growth. The hydrolysis of acetyl-CoA is coupled to the synthesis of adenosine triphosphate (ATP) [66]. The role of CODH in metabolism is extensive and beyond the scope of this review, but detailed reviews of acetogenic metabolism and the role of CODH/ACS have been written [1, 2, 67, 68]. The CODH/ACS has been purified from *Clostridium thermoaceticum* and *Acetobacter woodii* and characterized for enzyme size, subunits and metal content [69–71]. The enzyme is a tetramer with $\alpha_2\beta_2$ structure and contains 2 nickel atoms and ~ 10 iron atoms per $\alpha\beta$ dimer [69]. One nickel atom can be removed by chelation with 1,10-phenanthroline [72]. The nickel-chelated form of the enzyme maintains the CO-oxidation activity but loses the ACS synthase activity [73]. ACS catalytic activity can be partially reconstituted with the addition of nickel [72, 73]. Therefore, the two nickel sites and enzymatic activities are distinct.

Methanogenic bacteria convert acetate to methane and CO_2 and couple acetate degradation to ATP synthesis. This metabolic process uses the CODH/ACS enzyme (for reviews see [74, 75]). The CODH/ACS has been purified and has an $\alpha_2\beta_2$ structure with a large (80–90 kDa) subunit and a small (18–21 kDa) subunit [64]. All characterized methanogenic CODH/ACS enzymes contain nickel [64, 74]. Methane and CO_2 are formed by the ensuing process [64, 74]: (i) acetate is converted into acetyl-CoA by another enzymatic process [76–78]; (ii) acetyl-CoA binds to CODH/ACS and is cleaved into CoA, a bound CO and a methyl group [79, 80]; (iii) CoA is dissociated from the enzyme after cleavage; (iv) the methyl group is transferred to a tetrahydromethanopterin and then transferred to CoM [81]; (v) CoM reacts with methyl-CoM reductase, and methane is released (see following section); (vi) finally, the CO group is oxidized to CO_2, completing the reaction [74].

The structures of the nickel-iron-containing active sites of CODH/ACS have not been determined by X-ray crystallography. Spectroscopic analysis of the nickel-iron-containing active site has been extensive and will not be described here (for reviews see [1, 2, 64, 75]). A model for the two active sites has been proposed from

analysis of the spectroscopic data [62, 82]. Three metal clusters have been identified and are named the A-cluster, the B-cluster and the C-cluster. The A-cluster performs the acetyl-CoA synthesis reaction, the B-cluster is a typical Fe_4S_4 cluster involved in electron transfer and the C-cluster performs the CO-oxidation reaction. The A-cluster and the C-cluster both contain nickel and iron, and both clusters are proposed to comprise a nickel atom linked to an Fe_4S_4 cluster by a bridging ligand. The C-cluster is proposed to be very similar to the monofunctional CODH from *R. rubrum* [62]. The clusters have distinct properties that permit the different reactions to be performed.

Methyl-CoM reductase

As described in the previous section, the methanogenic Archaea grow anaerobically using an energy-conserving process called methanogenesis. The Archaea oxidize H_2 with a nickel-containing hydrogenase and use the electrons to reduce one to two carbon molecules (i.e. CO_2, formate, methanol, methylamine, CO and acetate) to methane [1, 3, 4, 83, 84].

Several pathways are used to reduce the various carbon substrates, including CODH/ACS, but all pathways converge to the common intermediate methyl-S-CoM (CoM is 2-mercaptoethane-sulfonate) [83, 84]. Methyl-CoM reductase is an enzyme that is common to all methanogenic pathways and is the final step in the reduction of the methyl group to methane. Methyl-S-CoM is a coenzyme involved in methanogenesis, as is a second unique methanogen coenzyme that is involved in the evolution of methane and is referred to as 7-mercaptoheptanoylthreonine phosphate (HS-HTP). A CoM-S-S-HTP disulfide forms as a product during the reduction of methyl-S-CoM. This CoM-S-S-HTP product is recycled by reduction by a separate enzyme, $F_{420}H_2$ dehydrogenase [85–87]. Methyl-CoM reductase contains nickel in a tetrapyrrolic structure called coenzyme F_{430}. All methanogens have F_{430}, and this cofactor is found exclusively in methanogens [83, 84].

Methyl-CoM reductase accounts for 10% of the cell protein, but two genetically distinct forms of the protein exist in the cell [88–91]. One form predominates during growth under limiting CO_2 and H_2, whereas the other form predominates during exponential growth. The two forms of methyl-CoM reductase possess distinct specific activities, amino terminal sequences, subunit sizes and charge properties. However, they contain identical F_{430} and subunit composition [83].

Methyl-CoM reductase and the F_{430} cofactor have been studied extensively by spectroscopic, analytical and biochemical methods (for reviews see [1, 4, 84, 92] and references therein). These works have had a major impact on the understanding of the enzyme. The X-ray crystal structure has confirmed many of the proposed models for methyl-CoM reductase. The three-dimensional structure of methyl-CoM reductase confirmed the $\alpha_2\beta_2\gamma_2$ structure predicted from previous work [4, 93]. The enzyme possesses two identical active sites, each containing an F_{430} cofactor and a nearby binding site for methyl-CoM and HS-HTP. When the coenzymes are bound, the active site pocket is very hydrophobic and would be ideal for radical-based enzyme catalysis. On this basis a radical-based mechanism was proposed for the reaction. The enzyme is activated when reduced to the Ni(I) oxidation state [94], which is consistent with the proposed mechanism [84].

Superoxide dismutase

In 1996 a nickel-containing superoxide dismutase (SOD) was identified in *Streptomyces* spp. IMSNU-1 and *Streptomyces coelicolor* ATCC 10147 [95]. The enzyme is a tetramer with 0.75 Ni atoms per subunit. The nickel-containing SOD differed from other known SODS (Fe, Mn and CuZn) by amino acid composition, N-terminal amino acid sequence and immunological response. EPR spectroscopy identified a Ni(III) species in the enzyme with a tetragonal geometry [95].

S. coelicolor contains two distinct SOD enzymes [96]. SOD1 contains nickel, and SOD2 is an FeZn-containing enzyme. SOD1 is induced by nickel, whereas SOD2 is repressed by nickel [96]. The gene for the nickel-SOD has been cloned from *S. coelicolor Muller* and named *sodN* [97]. SodN has no apparent sequence similarity to other known proteins. Nickel was shown to regulate transcription of SodN [97].

Glyoxalase I

Glyoxalase I from *E. coli* was overexpressed in *E. coli* and purified [98]. This purified glyoxalase I protein was not activated by zinc, the native metal in humans and yeast. Activation was achieved using Ni^{2+} with 1 mol of Ni^{2+} causing maximal activation of the enzyme. This is the first glyoxalase that functions with maximal activity with a metal other than zinc.

Isomerase

A putative Ni-binding cis-trans isomerase has been isolated by metal affinity chromatography [98a].

Mechanisms of nickel transport

Ni^{2+} transport by Mg^{2+} transport systems

Early reports that Ni^{2+} was transported into *E. coli* and *Enterobacter aerogenes* came from studies testing

the toxic effects of divalent metals [99]. The toxicity of the divalent metals was diminished when higher concentrations of Mg^{2+} were used, suggesting that the divalent metals were entering the cells through the Mg^{2+} transport system. Later work demonstrated that Ni^{2+}, Co^{2+} and Zn^{2+} were transported into the cells [100]. Mutants resistant to Co^{2+} were also resistant to Ni^{2+} [101]. These mutants required higher concentrations of Mg^{2+} to grow, and revertants that lost the requirement for higher Mg^{2+} concentrations also lost resistance to Co^{2+} and Ni^{2+}. The Mg^{2+} transport system was concluded to be the means of entry for Ni^{2+}. The organisms *Escherichia coli* and *Salmonella typhimurium* have been studied extensively for Mg^{2+} transport. In general, a constitutive system is expressed that will transport Mg^{2+}. Alternate systems with higher affinity for Mg^{2+} are expressed under low Mg^{2+} conditions. The biochemical and genetic characterization of Mg^{2+} transport systems that also transport Ni^{2+} will be briefly discussed.

CorA

In *E. coli*, mutant strains have been identified that are resistant to Co^{2+} (CorA and CorB). The resistance is attained by losing the ability to transport Co^{2+} [102]. Transport of Mg^{2+} in CorA and CorB mutants occurs by an alternate Mg^{2+} transporter that is expressed at low Mg^{2+} concentrations. Therefore, *E. coli* has at least two transport systems that transport Mg^{2+} and other divalent metals with different affinities.

Three Mg^{2+} transport systems (MgtA, MgtB and CorA) have been identified in *S. typhimurium* [103]. Mutant strains have been constructed that inactivate either each individual Mg^{2+} transport system, multiple systems or all three systems in order to characterize the properties of each system [104]. Each system transports Ni^{2+}, and due to the difficulty of obtaining the short-lived radioisotope $^{28}Mg^{2+}$, $^{63}Ni^{2+}$ was used as an analog for Mg^{2+} to study transport [105].

The CorA Mg^{2+} transporter is a constitutively expressed 40-kDa protein that has a K_m for Mg^{2+} of 20 μM and transports Mg^{2+} at high capacity [106]. The CorA protein has been identified in *S. typhimurium* and in *E. coli*, and the sequence is 98% identical [103]. CorA is not similar to any other sequenced protein and is a unique class of metal ion transporter. The CorA system performs both Mg^{2+} influx and efflux. CorA alone is sufficient to perform Mg^{2+} influx, but CorB, CorC, and CorD are required for efflux of Mg^{2+} at high Mg^{2+} concentrations [107]. The CorA system also mediates the influx of Co^{2+} and Ni^{2+} [103]. The CorA gene is widely distributed in gram-negative bacteria and functions as the constitutive Mg^{2+} transporter for many organisms [108].

The MgtA and MgtB systems

The MgtA and MgtB systems are P-type ATPase enzymes [109]. P-type ATPase transporters are phosphorylated on an aspartyl residue, and hydrolysis of the phosphate from the aspartyl residue completes transport [110]. P-type transport systems transport the biologically relevant cations Na^+, K^+, H^+, Mg^{2+} and Ca^{2+} in mammalian and bacterial organisms [110]. In *S. typhimurium*, MgtA and MgtB are induced by low Mg^{2+} concentrations and have slightly higher affinity for Mg^{2+} than CorA, with a K_m of 5 μM [105]. MgtA and MgtB both transport Ni^{2+} but do not transport Co^{2+}, and neither mediates Mg^{2+} efflux [111]. In general, eukaryotic and prokaryotic P-type ATPases differ in amino acid sequence and length and by hydropathy plots. The discovery that the P-type ATPase MgtB from *S. typhimurium* shows greater similarity to the eukaryotic genes allows it to be used as a model for eukaryotic P-type ATPases [109].

MgtE

A new Mg^{2+} transport system was identified in *Bacillus firmus* and *Providencia stuartii* [112]. This transport system confers sensitivity to Co^{2+} and also transports Ni^{2+}. The gene encodes a protein 34 kDa in size. The sequence of the gene showed no similarity to CorA or to other known transport proteins. Comparison between the genes from *B. firmus* and *P. stuartii* shows 75% identity, indicating the presence of a new class of Mg^{2+} transporter.

It is unclear if these systems play a functional role in delivering Ni^{2+} to the nickel-containing enzymes under natural growth conditions, because the affinity for Ni^{2+} by these systems is ~ 50 μM, whereas high-affinity Ni^{2+} transport systems have affinities of 17 nM–5 μM. An exception to this is *Clostridium pasteurianum*, which appears to transport Ni^{2+} under physiological conditions both by the nickel-specific transporter and by the Mg^{2+} transport system. The importance of understanding the Mg^{2+} transport systems occurs in the laboratory when studies are performed under high Ni^{2+} concentrations or when mutants lacking a high-affinity nickel transport system are studied. It is vital to understand the effect of the Mg^{2+} transport system under these conditions.

Ni^{2+} transport by Ni^{2+}-specific transport systems

Ni^{2+}-specific transport has been identified in a number of bacteria (for review see [113]). Some transport systems have been characterized genetically, and the proteins responsible for transport have been purified and characterized. In many of these organisms, only the Ni^{2+} accumulation data and kinetic data associated

with transport have been obtained: the proteins have not been purified, and the genes have not been identified. Below is a brief review of organisms that transport Ni^{2+} followed by a section describing the Ni^{2+} systems that have been characterized genetically.

Several acetogenic bacteria possessing the nickel-containing CODH have been studied for Ni^{2+} transport by Drake and co-workers. Ni^{2+} transport was energy-dependent and specific for Ni^{2+} in *Clostridium thermoaceticum* and *Acetogenium kivui* [114]. Kinetic analysis showed *C. thermoaceticum* and *A. kivui* have high affinity for Ni^{2+}, with K_m values for Ni^{2+} at 2.3 and 3.2 μM, respectively. Similar specificity for Ni^{2+} transport was also observed, as divalent metals did not inhibit transport.

Several other systems have been identified that have very unique characteristics for Ni^{2+} transport. *C. pasteurianum* exhibited (i) lower affinity for Ni^{2+} with a K_m of 85 μM; (ii) inhibition of nickel transport by divalent metals; (iii) energy-dependent transport of Ni^{2+} [115]. Transport of Ni^{2+} was concluded to occur by the magnesium transport system and by another system that was not inhibited by Mg^{2+}. The cyanobacterium *Anabaena cylindrica* possesses an energy-dependent high-affinity Ni^{2+} transport system that transports Ni^{2+} with a K_m of 17 nM [116]. Other organisms appear to have Ni^{2+} transport systems that are not as dependent on energy. *Azotobacter chroococcum* appears to transport Ni^{2+} in an energy-independent fashion [117]. An energy-independent adsorption of Ni^{2+} to the cell surface and cell sheath is responsible for Ni^{2+} accumulation in *Methanothrix concilii* [118]. Ni^{2+} transport by *Methanobacterium bryantii* is done with high-affinity (K_m of 3.1 μM), selectivity and requires energy, but not from ATP. The energy requirement appears to come from a proton gradient [119]. Finally, Ni^{2+} transport in *Bradyrhizobium japonicum* was Ni^{2+}-selective but lower affinity than most Ni^{2+} specific transport systems (K_m 25 and 50 μM for two systems reported). The transport of Ni^{2+} was not inhibited very significantly by any metabolic inhibitor, leaving the energy requirement unclear [120].

Genetically characterized Ni^{2+} transport systems

Two classes of high-affinity nickel transport systems have been genetically identified. The first class is the single-component transport system such as HoxN, HupN, UreH and NixA. The second class is the multicomponent ATP-dependent class of transporters represented by NikABCDE and the ABC transporter of *Helicobacter pylori*.

HoxN

The HoxN gene was found in the hydrogenase gene cluster of *Alcaligenes eutrophus* [121]. HoxN is a 33-kDa protein with eight predicted membrane-spanning regions and functions as a single-component ion carrier of Ni^{2+} [122, 123]. HoxN permits growth on 100 nM Ni^{2+} concentrations and is not affected by Mg^{2+}. HoxN-type transporters are specific and have $K_m \sim 10–20$ nM with low capacity for transport [123].

HupN

The gene for HupN is found in *Bradyrhizobium japonicum* on an operon with the genes for HupO and HupP [124]. HupN is a 40-kDa protein that shows 56% identity to HoxN from *A. eutrophus*. The *hypN* gene alone partially complements mutants in nickel transport. Combined with HupO and HupP, it completely complements nickel transport for hydrogenase activity.

UreH

Sequencing of the urease operon in *Bacillus* sp. strain TB90 identified the typical urease operon of *ureABCDEFG* but also included two more genes, *ureH* and *ureI*. UreH showed 23% amino acid identity to HoxN of *A. eutrophus*. The similarity of UreH to HoxN prompted the authors to speculate that UreH has a role in Ni^{2+} transport [125].

NixA

H. pylori urease, expressed in *E. coli*, required supplemental Ni^{2+} for urease activity [126]. In vivo, *H. pylori* does not require exogenously added Ni^{2+} for urease activity. It was assumed that a nickel transport system was responsible for making Ni^{2+} available for urease in native *H. pylori*. Screening of a library of *H. pylori* in *E. coli* containing the urease structural genes identified a clone that contained DNA exhibiting urease-enhancing activity [126]. The gene was sequenced and identified as *nixA*, which encodes a 34-kDa integral membrane protein. Insertion mutations into *nixA* abolished the urease activity, indicating that the NixA protein functions as a Ni^{2+} permease. NixA is a high-affinity Ni^{2+} transporter with a V_{max} of 1750 pmol Ni^{2+}/min/10–8 cells and a $K_m = 11.3$ nM. Although Ni^{2+} transport is considered to be Ni^{2+}-specific, NixA is inhibited by Co^{2+}, Cu^{2+} and Zn^{2+} [127]. NixA is predicted to have eight transmembrane-spanning regions. Three homologs of NixA have been identified and are HoxN of *A. eutrophus*, HupN from *B. japonicum* and UreH from thermophilic *Bacillus* TB90. Other putative nickel transport proteins are

HupE from *Rhizobium leguminosarum bv. viciae* [128] and UreJ from *Bordetella bronchiseptica* [129].

ABC transport of *H. pylori*

NixA deletion mutants still retained urease activity, indicating the presence of an alternate nickel transport system. Nucleotide sequence analysis of *H. pylori* revealed a homolog of NikD that is a component of the ATP-dependent nickel transport system in *E. coli* (see below). Further work identified the *abcABCD* genes, and *abcC* was similar to the ATP-binding protein of an ABC transport system. The other genes do not have significant sequence similarity to other database proteins. Further analysis is required to confirm a role in nickel transport, but mutations in *abcCD* decreased urease activity [130].

NikABCDE

E. coli contains a nickel transport system composed of five gene products that show similarity to other bacterial periplasmic transport systems [131]. The *nikABCDE* genes have been shown to be regulated by a nickel-responsive regulator, NikR [132]. The ATP-binding cassette family of transporters transports sugars, amino acids, peptides and inorganic ions [133]. These systems are made up of a periplasmic substrate-binding protein, integral membrane proteins that form the permease, and multiple cytoplasmic proteins that bind and hydrolyze ATP, providing energy for the transport process. NikA is the periplasmic binding protein, NikB and NikC are integral membrane proteins, and NikD and NikE possess typical ATP binding domains to couple transport to ATP hydrolysis. NikA has been purified and characterized and binds 1 Ni^{2+} atom per molecule with a K_d of 0.1 μM [134].

Other divalent metal transporters

Several other divalent metal transport systems have been reported. A Co^{2+}-specific transport system has been identified in *Rhodococcus rhodochrous* and is similar to the HoxN family of Ni^{2+} transporters [135]. Mn^{2+}-specific transport systems have also been reported [136].

Nickel-processing systems

The nickel enzymes, urease, hydrogenase and CODH from *Rhodospirillum rubrum* have all been purified in a nickel-deficient, inactive form. Attempts to reconstitute enzyme activity by the addition of nickel have shown these enzymes are very difficult to activate. Purified apo-hydrogenase has not been activated, apo-urease has been activated to low levels of activity after long incubations with Ni^{2+} and apo-CODH from *R. rubrum* can only be activated to full activity with a powerful reductant and nonphysiological concentrations of Ni^{2+}. All of these observations suggest that an in vivo mechanism exists for assembly of the nickel active site.

Nickel-processing systems have been identified by studying mutants that produced nickel-deficient forms of the studied nickel enzyme or by mutationally inactivating genes encoding accessory proteins in operons coding for nickel enzymes. The mutations in genes for accessory proteins have resulted in the production of inactive nickel-deficient enzymes. Two common motifs have been identified from sequence comparisons among nickel accessory proteins involved in nickel insertion into nickel-containing enzymes: a nucleotide binding motif (P-loop), and a histidine-rich region (nickel binding domain). The current knowledge of accessory proteins involved in nickel insertion to nickel enzymes will be reviewed below. The nickel-processing proteins from the characterized systems are summarized in table 1.

Table 1. Properties of nickel processing proteins.

Characteried functions and motifs	Proteins with the indicated motif or required for indicated function		
	hydrogenase	urease	CODH
Nucleotide binding motif	HypB, HypF	UreG	CooC
Nucleotide binding demonstrated	HypB	UreD, UreF, UreG	ND*
Histidine-rich motif	HypB†	UreE†	CooJ
Nickel binding demonstrated	HypB	UreE	CooJ
Proteins that bind to the Ni enzyme	HypC	UreD, UreF, UreG	ND
Regulation of Ni enzyme expression	HypA, HypB, HypF	ND	CooA
Iron sulfur or zinc-finger motif	HypA, HypF	ND	CooC?
Nickel transport systems	NikABCDC‡	NixA§	ND

* Not determined.
† Not all *hypB* and *ureE* genes encode a histidine-rich region for HypB and UreE.‡ The NikABCDE transport system is in *E. coli*.
§ The NixA protein is found in *Helicobacter pylori*.

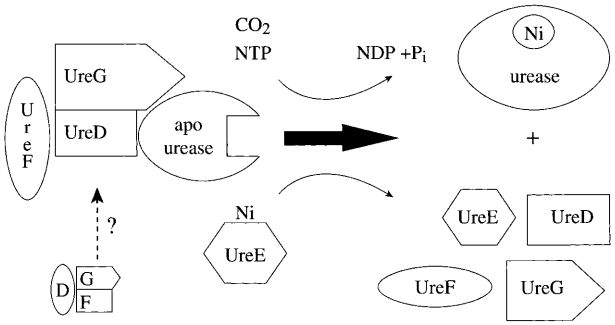

Figure 3. Model for Nickel Insertion into Apo-urease. UreD and UreF bind to the apo-urease and hold it in a conformation that binds CO_2 and Ni^{2+}, producing enzymatically competent urease. UreG forms a complex with UreD and UreF and may assist in the binding of these proteins to the apo-urease. A complex with UreD-UreF-UreG-apo-urease has been identified and is proposed to be the in vivo complex that inserts Ni^{2+} into apo-urease. UreE is a nickel-binding protein and is proposed to bind and deliver Ni^{2+} to the UreD-UreF-UreG-apo-urease complex for Ni^{2+} insertion. A nucleotide triphosphate (ATP or GTP) is proposed to be hydrolyzed to insert Ni^{2+} into apo-urease, or to dissociate the protein complex after Ni^{2+} has been inserted. Adapted from the model of Hausinger [18].

Urease

The majority of the work characterizing urease genes and proteins involved in nickel processing has been conducted in *K. aerogenes*, *Proteus mirabilis* and *H. pylori* [137–141]. An excellent review of nickel processing systems has been written by Hausinger [5]. The urease operon contains the following genes, *ureD-ABCEFG* [141]. The structural genes encoding the urease enzyme are *ureABC*. The other genes, *ureDEFG*, are proposed to function in nickel insertion into apo-urease [141]. Lee and Hausinger demonstrated that knockout mutations in *ureD*, *ureF* and *ureG* produce nickel-deficient urease, although urease expression is not affected [142]. Strains with knockout mutations of *ureE* produce urease with lowered activity and diminished nickel content [142]. The *ureDEF* genes are poorly conserved among various urease gene clusters and show limited or no similarity to other genes in database searches [18, 143]. The work characterizing the roles of *ureDEFG* is described below. A model developed by Hausinger and co-workers for the actions of these proteins is shown in figure 3.

Activation of Apo-urease

Nickel-deficient (apo-urease) can be obtained when *K. aerogenes* cells are grown on nickel-depleted medium [144]. Apo-urease is activated in vivo by addition of Ni^{2+} to the growth medium. Cultures of *K. aerogenes* containing apo-urease were activated when nickel was added to the culture, even when inhibitors of protein synthesis were present. This indicates that nickel insertion does not occur during protein folding but is a posttranslational event. When cultures containing apo-urease were treated with dinitrophenol (a protonophore) or dicyclohexylcarbodiimide (ATPase inhibitor), no activation occurred upon addition of nickel to the culture [144]. This observation indicates the requirement for energy in the nickel insertion process. Deletion mutants of accessory proteins in the urease operon produced apo-urease in vivo, indicating the role of these genes in nickel insertion into urease [141].

Purified apo-urease is activated very poorly by the addition of Ni^{2+} to the purified protein [144]. In vitro activation of apo-urease was first observed by adding Ni^{2+} to extracts of *E. coli* grown in nickel-depleted medium that overexpressed the urease genes from *K. aerogenes* [145]. The addition of Ni^{2+} to these extracts activated urease 10% after 1 day. Incubation of carbon dioxide with apo-urease prior to the addition of Ni^{2+} permitted a greater extent of activation [146]. The observed activation with carbon dioxide was complete in 3 h, and 30% of the enzyme present was activated.

Increased activation has been achieved in the presence of some of the nickel-processing proteins for urease. The current understanding of the function of the urease nickel insertion proteins is discussed below and represented in figure 3.

UreD

The *ureD* gene is required for Ni^{2+} insertion into urease, but analysis of the UreD sequence reveals no recognizable motifs [142]. When the *K. aerogenes* urease gene cluster is overexpressed in *E. coli*, UreD copurifies with the apo-urease enzyme (UreABC) on native gels [145]. Several complexes were observed on native gels that were identified as apo-urease (UreABC) complexed with one, two, or three UreD molecules. The addition of nickel to UreD-apo-urease complexes resulted in rapid activation of the enzyme in 1 h. The activation correlated with the number of UreD molecules present, with maximal activation occurring with three UreD molecules bound per apo-urease trimer. Activation under these conditions activated urease to a specific activity of 30% compared with fully active urease. The activation process was accompanied with the dissociation of the UreD protein from the urease enzyme. UreD is proposed to be a chaperonin protein that holds urease in a conformation that allows Ni^{2+} to enter [145]. Further study showed that Ni^{2+} binds to the apo-urease in an inactive form [147]. The presence of UreD and

CO_2 increases the likelihood that Ni^{2+} binds in an active conformation. Other divalent metals were shown to bind to apo-urease and UreD:apo-urease proteins with higher affinity than Ni^{2+}. This observation suggests that the role of the accessory proteins may be to convey specificity for Ni^{2+} or to reverse the inappropriate binding of competing metals or nonproductively bound Ni^{2+} [147].

UreE

The UreE protein is proposed to bind Ni^{2+} and to facilitate the insertion of nickel into urease [141]. UreE has been purified and characterized from several organisms. Sriwanthana et al. demonstrated that ^{63}Ni coeluted with a heterologously expressed UreE protein from *P. mirabilis*, suggesting that UreE binds nickel in vivo [148]. The *K. aerogenes* UreE, which contains 10 His residues in the final 15 amino acids, binds six Ni^{2+} per dimer with a K_d of 9.6 μM. Spectroscopic analysis of UreE by EXAFS and variable temperature magnetic circular dichroism showed a pseudo-octahedral coordination of the nickel ions [149]. The location of UreE is cytoplasmic as judged by immunogold electron microscopy. Brayman and Hausinger observed that *ure*E genes from several organisms lack the histidine-rich region. To study the role of the histidine-rich region, the *ureE* gene was truncated immediately before the start of the histidine-rich region (final 15 amino acids). The truncated protein was called H144*UreE [150]. The *K. aerogenes* urease operon, containing either the wild-type UreE, the H144*UreE or UreE deletions, was heterologously expressed in *E. coli* and was tested for urease activity. Cells containing H144*UreE showed 73% of the urease activity of wild type but were 10–13% more active than cells containing UreE deletions. The histidine-rich region of UreE was not required for protection against nickel toxicity, as the strain with H144*UreE showed growth identical to the strain with the wild-type UreE in medium containing 3 mM $NiCl_2$. The H144*UreE was purified by immobilized metal affinity chromatography (IMAC) chromatography and was shown to cooperatively bind 1.9 nickel ions per dimer. The authors note that organisms possessing high-affinity nickel-uptake systems do not have nickel-binding motifs in UreE, but organisms that have no uptake systems have histidine-rich regions. The authors proposed that the histidine-rich region may be used for nickel storage [150]. This work was extended by identifying several of the residues that are involved in this internal Ni^{2+} binding site. The two internal binding sites are proposed to be at the interface of the UreE dimer; His-96 and Asp-11 are two residues required for binding of the first equivalent of Ni^{2+}. These two residues are highly conserved among UreE proteins from various organisms [151].

UreF

The UreF protein is the least-characterized accessory protein. UreF is predicted to be a cytoplasmic protein. Limited activation of urease was observed in extracts from *ureF* mutants [145]. UreF may assist the formation of the UreD-apo-urease complex [152]. A complex made up of UreD-UreF and apo-urease was observed [153] and demonstrated activation properties very different from the UreD-urease complex previously characterized [147]. The UreD-UreF-urease complex was resistant to forming inactive Ni^{2+} complexes and had a significantly decreased dependence on bicarbonate [153]. The activity was approximately 30% of the specific activity of wild-type enzyme. Immunoblots of the UreD-UreF-apo-urease complex from a native gel did not cross-react with UreD. The authors concluded that UreF binds on top of UreD and covers the antigenic regions that react with the antibodies. UreF was proposed to bind and modulate the UreD-urease complex activation properties, including the exclusion of Ni^{2+} from the active site until the carbamylated lysine formed properly [153]. Recently, the urease gene cluster from *Bordetella bronchiseptica* was characterized, and the genes encoding UreE and UreF were fused, producing a UreEF protein [129]. It was proposed that this fusion conferred tighter coordination on the nickel donation, requiring that the lysine be carbamylated prior to nickel binding.

UreG

The UreG protein is the most highly conserved accessory protein among the urease gene clusters characterized [143]. UreG contains a nucleotide binding motif or P-loop. The *P. mirabilis* UreG protein has limited sequence similarity to a 60-kDa chaperonin of thermopholic bacterium ps-3 [154]. UreG also has similarity to the HypB protein involved in nickel insertion into nickel-containing hydrogenases [143].

Knockout mutations of the *ureG* gene produce a nickel-deficient form of urease [141]. However, extracts of *ureG* mutants can be partially activated by the addition of Ni^{2+} in vitro [143]. The UreG protein has been isolated and characterized as a monomer of 21.9 kDa [155]. Purified UreG did not bind or hydrolyze ATP or guanosine triphosphate (GTP) and had no affinity for ATP or GTP chromatography resins. Mutations to the P-loop produced an inactive form of urease in vivo, indicating the essential requirement for a functional P-loop in vivo. A complex made up of UreD-UreF-UreG-apo-urease has been previously identified [152], and mutations to the P-loop abolish the formation of this complex [155]. In cells containing mutations in the urease structural genes and the *ureE* gene, an insoluble complex containing UreD, UreF and UreG (named the

DFG complex) was identified. This complex can be solubilized in 0.5% Triton and binds to ATP-linked agarose resins. Mutations to the P-loop form the DFG complex, but this complex does not bind to ATP-linked agarose resins. This indicates that UreG requires UreD and UreF in order to bind and to hydrolyze nucleotides for the insertion of Ni^{2+} into urease [155].

UreH

The *ureH* gene is unique to the urease operon from *Bacillus* TB-90. The *ureH* gene encodes a protein that is similar to the HoxN protein from *A. eutrophus*. The HoxN protein is a high-affinity nickel transport protein that was discussed in the Ni^{2+} transport section.

Figure 3 represents a model of current knowledge about urease metallocenter assembly. UreD is known to hold the apo-urease in an open conformation to aid in Ni^{2+} binding. UreF binds on top of UreD and appears to protect the enzyme from incorrect binding of the Ni^{2+} atoms to the carbamylated lysine residue. UreG contains the nucleotide binding domain and binds nucleotides when in a complex with UreD and UreF. It is not clear whether UreDFG form a complex and then bind to apo-urease or whether UreD binds apo-urease followed by the binding of UreF and UreG. UreE is the nickel binding and delivery protein that supplies the complex with Ni^{2+}. Hydrolysis of nucleotide is postulated to insert Ni^{2+} into urease or to be required to dissociate UreDFG after Ni^{2+} has been properly inserted.

Hydrogenase

The identification of a nickel-processing system for hydrogenase was aided by the isolation of mutant strains with defects in the maturation of all three *E. coli* hydrogenases [156]. The mutations map to the 58–59 min region of the *E. coli* chromosome [157, 158]. The region has been sequenced and contains five genes designated as *hypABCDE* with another gene, *hypF*, found separately. Operons similar to the *E. coli hyp* operon have been identified in other organisms [159]. Strains with mutations in the *hyp* operon accumulate immature forms of the large and small subunits of hydrogenase, and therefore the role of these gene products is proposed to be in maturation of the enzyme into an active form [159].

The genes encoding the structural proteins of the hydrogenase enzymes have been identified and sequenced from many organisms (for review see [159]). The operons encoding the structural genes have other genes that encode accessory proteins (*hupC*, *hydC*, *hoxZ*, *hyaC* and *hybB*), but these proteins are not related to nickel insertion (for review see [159]). They are proposed to function in anchoring the hydrogenase proteins to the membrane and to serve as electron transport carriers to the membrane-bound hydrogenase (for review see [159]).

A proposed model for nickel incorporation into hydrogenase is shown in figure 4. Both the large and small subunits are synthesized in precursor forms that are proteolytically cleaved as the maturation of the active hydrogenase proceeds [160]. The proteolytic cleavage of the *E. coli* large subunit of hydrogenase 3 is performed by the specific protease HycI. Mutations in *hyp* genes produce a nickel-deficient form of the noncleaved large subunit, indicating that nickel insertion into hydrogenase is required before proteolytic cleavage [161]. Mutations in the *hycI* gene produced a precursor of the hydrogenase subunit that contained stoichiometric amounts of ^{63}Ni [161]. Therefore, it is proposed that nickel insertion precedes proteolytic processing.

The hyp operon

The *hyp*B gene products are known to play a role in processing nickel for the Ni-Fe hydrogenases of *E. coli*, *Azotobacter vinelandii*, the *Rhizobia* spp. and related organisms [159]. Deletions in the *hypB* gene result in a nickel-deficient hydrogenase [156], but *hypB* mutations can be overcome by high nickel concentrations (500 μM) [158]. The *hyp*B genes have sequence similarity to portions of both the *cooC* and *UreG* genes (P-loop) and to the *cooJ* and *ureE* genes (nickel binding motif). The

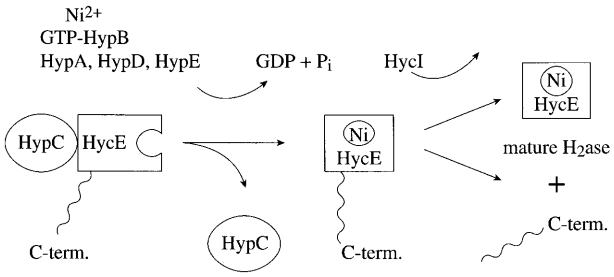

Figure 4. Nickel Insertion Model for Hydrogenase. The HypC protein has been shown to bind to the large subunit of the hydrogenase enzyme (HycE) and to hold HycE in a conformation able to accept Ni^{2+}. The HypB protein has been shown to bind and hydrolyze GTP. HypB is proposed to couple the energy released from the hydrolysis of GTP to insert Ni^{2+} into the apo-HycE protein. HypC does not bind to the nickel-containing form of the pre-HycE protein and is shown dissociating from HycE after Ni^{2+} is inserted. The C-terminus of HycE is cleaved by HycI, and this cleavage is proposed to make the insertion of Ni^{2+} irreversible.

*E. coli hyp*B gene does not encode a histidine-rich region [157]. HypB shares 23% sequence identity to UreG [159]. HypB proteins have been purified and characterized from *E. coli* [39], *Rhizobium leguminosarum* [162] and *B. japonicum* [163]. HypB from *E. coli* is a homodimer that binds guanosine diphosphate (GDP) and catalyzes the hydrolysis of GTP but does not bind nickel [39]. HypB from *R. leguminosarum* was found to bind 3.9 Ni^{2+} atoms per HypB monomer with a K_d of 2.5 μM, but no GDP binding or GTP hydrolysis was observed [162]. The *B. japonicum* HypB binds 9.0 Ni^{2+} atoms per monomer with a K_d of 2.3 μM and catalyzes the hydrolysis of GTP [163]. Maier and Böck proposed that HypB interacts with the hydrogenase apo-protein in the presence of other components required for nickel insertion into hydrogenase, and that GTP hydrolysis would release the HypB protein from the complex after nickel was inserted [39]. HypB was shown not to be required for nickel transport into the cell, as a HypB mutant strain was able to incorporate nickel into *E. coli* containing the *K. aerogenes* urease operon [156].

The roles of other *hyp* genes are not well defined. Mutational analysis has demonstrated that *hypB*, *hypD*, *hypE* and *hypF* appear to function in the activation of all three hydrogenases in *E. coli*, signifying a general role in hydrogenase maturation [159]. The *hypA* and *hypC* genes are required only for correct maturation of hydrogenase 3 [156]. HypA has a regulatory function for both the *hyp* operon and the *hyc* operon and acts as a repressor for the *hyb* operon [160]. HypC is essential for the generation of hydrogenase 3 activity and enhances the activity level of hydrogenase 1 [160]. HypA and HypF have typical motifs reminiscent of iron-sulfur proteins and zinc-finger proteins [159]. HypF has a histidine-rich region [HHH(A/D)H] that may assist in nickel binding during the insertion process [159]. HypF has been shown to regulate the synthesis of HupL protein in *Rhodobacter capsulatus* [164] and the insertion of nickel into HycE in *E. coli* [165]. HypC was demonstrated to bind to the unprocessed large hydrogenase subunit (HycE) in *E. coli*, but not to the processed form of HycE. This observation is consistent with a role in binding to the HycE protein and holding it into a conformation accessible for metal incorporation [166].

Figure 4 summarizes the known data for Ni^{2+} insertion into apo-hydrogenase. Apo-hydrogenase (HycE) is held in an open conformation by HypC. HypA, D and E are all required; their functions are not yet defined, but may play roles in iron insertion or in the assembly of the CO or CN^- ligands at the active site [167]. HypB appears to function as a Ni^{2+} binding and delivery protein and also couples the hydrolysis of nucleotide (GTP) to insert the Ni^{2+} atoms or to dissociate the protein complex from the enzyme.

In vitro activation of hydrogenase

Activation of hydrogenase 3 from *E. coli* has been obtained, and the activation accounts for approximately 12% of the total hydrogenase present [168]. The activation was achieved by adding Ni^{2+} (400 μM) to an extract from a strain containing mutations in the *nik* operon. Mutation in the *nik* operon led to the formation of a nickel-deficient precursor form of HycE. The in vitro reaction occurred only under anaerobic conditions and in the presence of HypB, HypC, HypD, HypE, HypF and HycI, which are *hyp* accessory proteins. The HycE protein, which is a specific protease required for cleavage of the C-terminal tail of HcyE, was also required for hydrogenase activity.

Other hydrogenase accessory proteins

HupK from *R. leguminosarum* is similar to the large subunit of the hydrogenase and has conserved nickel binding motifs that are altered slightly [169]. This protein is proposed to act similarly to the NifNE proteins from nitrogenase that function as scaffolds for the assembly of the metallocluster [170].

HupUV and HoxBC

Hydrogenase-like sensor proteins have been discovered in *R. capsulatus* and *A. eutrophus*. These proteins, which have significant sequence similarity to hydrogenases, exhibit very low hydrogenase activity. Genetic and physiological analyses indicate that these proteins serve as sensors involved in the control of hydrogenase expression. HupUV from *R. capsulatus* has been characterized by Vignais et al. [170a]. The *hoxbc* genes have been characterized in the Friedrich laboratory and characterized spectrally [170b].

CODH of *R. rubrum*

The genes encoding CODH, the CO-tolerant hydrogenase and the ferredoxin-like protein (CooF) have been cloned and sequenced [171–174]. By sequencing the DNA adjacent to the gene encoding CODH (*cooS*), two complete operons (*cooFSCTJ* and *cooMKLXUH*) as well as the gene encoding the activator protein (CooA), which induces expression of the CO-oxidation system, have been identified. A model of the gene arrangement for the sequenced region of DNA encoding the CO-oxidation system is shown in figure 5. The present understanding of the *coo* gene products is discussed below.

CooA

The *cooA* gene encodes a protein, CooA, which regulates the expression of the CO-oxidation system [174].

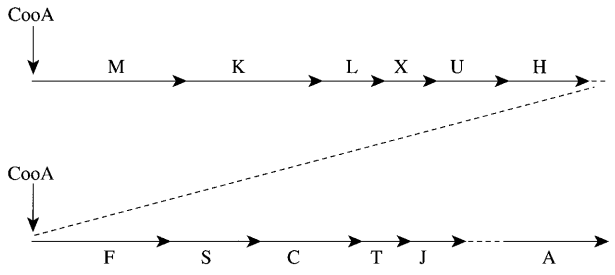

Figure 5. The *coo* operons encoding the CO-oxidation system of *R. rubrum*. The first operon encodes the hydrogenase genes *cooMKLXU* [173]. The second operon, *cooFSCTJ*, encodes CODH, the ferredoxin-like protein CooF, and the nickel processing proteins CooC, CooT and CooJ [171, 172]. CooA binds upstream of each operon and initiates expression of the gene [173, 177].

The *cooA* gene is adjacent to the operon encoding the *cooFSCTJ* genes. A deletion of *cooA* produces a mutant that fails to express the CO-oxidation system in the presence of CO. The *cooA* mutation can be overcome when a plasmid carrying *cooA* is introduced into the mutant strain. CooA is similar to members of the cyclic AMP receptor protein (CRP) family and to FNR of *E. coli* [174].

CooA has been purified and shown to be a dimeric, heme-containing protein that binds to DNA after binding CO [175, 176]. CooA regulates the transcriptional start sites for the *cooFSCTJ* and for *cooMKLUXH* genes. CooA binding to the DNA was demonstrated by DNase I footprinting for *cooFSCTJ* [177] and *cooMKLUXH* [173]. The CooA binding site had twofold symmetry (5′-TGTCA-N_6-CGACA) that is similar to the motif recognized by the CRP/FNR family [177].

When *R. rubrum* is exposed to CO, CooA binds CO and is presumed to undergo a conformational change allowing binding to DNA. CooA binding upstream of the *cooFSCTJ* and *cooMKLUXH* operons induces expression of CODH (*cooS*) and the CO-tolerant hydrogenase (*cooLH*) along with the other required components of the CO-oxidation system.

The operon encoding the CO-tolerant hydrogenase shows no gene similarity to the nickel-binding proteins but has proteins similar to the small and large subunits of nickel-containing hydrogenases. Other proteins similar to the NADH ubiquinone oxido reductase of *E. coli* oxido reductase were found, and Fox et al. speculate that these gene products are involved in translocation of protons to produce energy [173].

The operon encoding CODH

The operon encoding CODH contains five genes, *cooFSCT and J*. The *cooF* gene product (CooF) encodes the ferredoxin-like protein that transfers electrons from CODH to the CO-tolerant hydrogenase. The *cooS* gene encodes CODH. The *cooCTJ* genes encode proteins required for the insertion of nickel into CODH [178].

The *cooCTJ* genes are similar to some of the nickel-processing genes from the nickel-containing enzymes hydrogenase and urease. Deletion of *cooCTJ* genes results in the production of a nickel-deficient CODH, confirming a role in nickel processing. The nickel-deficient CODH purified from a *cooCTJ* mutant can be completely activated in vitro by the addition of reductant and Ni^{2+}. The ability to activate CODH from a *cooCTJ* mutant indicated that the mutation affected only the in vivo insertion of nickel into CODH.

The *cooC* gene encodes a 27.8-kDa protein predicted to contain a P-loop, or nucleotide binding domain [172]. CooC shows similarity to the HypB and UreG proteins involved in nickel insertion into hydrogenase and urease, respectively. NifH, involved in assembly of FeMo-co for nitrogenase, also shows similarity to CooC. Mutant strains lacking a functional *cooC* gene require 550 μM $NiCl_2$ supplementation to grow on CO [172]. The presence of the P-loop in HypB, UreG and CooC indicates that nucleotide hydrolysis is required for nickel insertion in vivo [39].

The *cooT* gene encodes a 7.1-kDa protein that shows marginal overall similarity to the HypC protein family [172]. The *hyp* operon encodes a series of genes in *E. coli* that are required for the production of all three nickel-containing hydrogenases [179]. The *hypC* gene is essential for hydrogenase formation in *E. coli* and *A. eutrophus* [159]. Insertion mutations disrupting the reading frame of CooT showed a weak phenotype exhibiting slightly better growth on CO than wild-type cells [172].

The *cooJ* gene encodes a soluble, 12.6-kDa protein that contains a C-terminal region containing 16 histidine residues in the final 34 amino acids [172]. The histidine-rich region is a nickel-binding motif. CooJ has been purified and characterized and binds 4.0 Ni^{2+} per monomer with a K_d of 4 μM. CooJ selectively discriminates for Ni^{2+} vs. all divalent metals tested except for Zn^{2+} that bound with equal affinity to Ni^{2+} [180]. Most UreE and HypB proteins contain nickel-binding motifs [150] and have been shown to bind nickel in vitro [149, 162, 163]. This class of proteins has been proposed to function as nickel-binding and delivery proteins.

At present the model for Ni^{2+} insertion into apo-CODH is based on the proposals for analogous systems for hydrogenase and urease. In this model, CooC acts as a nucleotide-hydrolyzing enzyme to couple energy to insert the Ni^{2+} and CooJ functions to bind and deliver Ni^{2+} to apo-CODH. The observation that CODH can

be activated in vitro suggests that the Ni^{2+} site may be more easily accessed and does not require a chaperonin-like protein such as UreD or HypC to hold it in an open conformation to bind nickel. This may explain the lack of a UreD or HypC analog in the *R. rubrum coo* operon.

The proposed functions for the nickel-processing proteins are heavily based on the intermediate complexes that have been observed for apo-urease in *K. aerogenes*. An alternate model may be considered where the Ni^{2+} that enters the cell is bound in an inaccessible form for the apo-enzymes. *B. japonicum* has a protein that binds Ni^{2+} in a form that does not exchange with free Ni^{2+} [181]. Ni^{2+} has also been observed in polyphosphate bodies [182] that may be inaccessible to the apo-enzymes of urease, hydrogenase and CODH. Such tight binding of Ni^{2+} may protect the cell from the toxic effects of Ni^{2+} but may also make it inaccessible for apo-nickel enzymes. The nickel-processing proteins may function to liberate the Ni^{2+} from the inaccessible storage locations for use in nickel enzymes.

Other nickel-processing systems

Analogs of CooC from organisms containing CODH/ACS enzymes

Sequence alignment programs have been used to identify several putative CooC analogs from organisms containing CODH/ACS enzymes. ORF1 from *Methanosarcina thermophila* is 57% similar to CooC and is found in the *cdh* operon encoding other CODH/ACS proteins [183]. Another protein (MJ0823) from *Methanococcus jannaschii* is 63% similar to CooC [184].

SOD and methyl-CoM reductase

No genes for nickel processing have been reported for nickel-containing SOD. Since nickel regulates the expression of *sodN* [97], the presence of a nickel transport system and sensor of nickel is likely. Similarly, no processing genes have been reported for methyl-CoM reductase, but related systems for transport and sensing of nickel are probable [185].

GroEL and GroES

The GroEL and GroES proteins appear to function in the activation and stability of urease from *H. pylori*. The GroEL and GroES proteins function as chaperonins that stabilize proteins during folding and during stresses to the cell. The urease from *H. pylori* is a prominent extracellular cell-bound enzyme that is tightly associated with a 58–62 kDa protein [139, 186]. The 58–62 kDa protein was identified as a GroEL protein (HspB). The GroEL protein is postulated to stabilize the urease complex in the acidic environment of the stomach [187]. Urease enzyme activity has been postulated to be the cause of the virulence by *H. pylori* [139, 187]. GroEL has been cloned, and the gene encoding GroEL (*hspB*) has been identified [188]. The regulon was shown to be bicistronic and also encoded the *hspA* gene that in turn encodes a protein similar to GroES. HspA contained a nickel binding motif in the C-terminus. A second HspA protein was found in *H. pylori*, indicating that this HspA protein may be specific for urease interaction. It is interesting to observe that the UreE protein in *H. pylori* does not contain a nickel binding motif [188]. HspA was purified and shown to bind two Ni^{2+} atoms per monomer with a K_d of 1.8 μM [189]. Coexpression of *hspA* and the urease operon in *E. coli* showed increased urease activity [188]. Although a role for Ni^{2+} binding or delivery to urease is speculated for HspA, no interaction between HspA and urease has been demonstrated [190].

A role for GroE proteins in metal insertion into hydrogenase has also been proposed [191]. Hydrogenase was decreased 60% in GroEL and GroES heat-sensitive strains of *E. coli*. These mutations caused a complete loss of HYD1 activity, had very little effect on HYD2 activity and resulted in an increased accumulation of the precursor form of the large subunit of HYD3. Increasing the concentration of Ni^{2+} did not suppress the mutations, indicating that Ni^{2+} insertion was affected by the mutations. GroEL was also demonstrated to bind to the precursor form of the large subunit of HYD3 in vitro. It was concluded that the GroE proteins assisted in the insertion of Ni^{2+} into the hydrogenase proteins [191].

Conclusions

In summary, Ni^{2+} is transported into the cell, generally by high-affinity Ni^{2+} transport systems; however some Ni^{2+} may enter through the Mg^{2+} transport systems of the cell. Once Ni^{2+} enters the cell, the Ni^{2+} is bound by a Ni^{2+}-binding protein that is proposed to protect the cell from free Ni^{2+}. This protein is proposed to deliver the Ni^{2+} to the appropriate apo-enzyme. A common requirement for a protein containing a nucleotide binding domain (P-loop) and a histidine-rich region (nickel binding domain) exists among the characterized nickel-processing systems of hydrogenase, urease and CODH. The number of accessory proteins required for nickel insertion into urease and hydrogenase is larger than required for the *R. rubrum* CODH. This may be due to the complicated nickel active sites of these proteins. Extra accessory proteins may be required for the carbamylation of lysine in the urease system and for CN^-

and CO ligation to iron in hydrogenase. Therefore, extra gene products are required for nickel insertion into urease and hydrogenase that are not required for CODH. The chaperonins GroEL and GroES may also be involved in holding the Ni enzymes in a conformation that allows Ni to be inserted.

1 Ragsdale S. W. (1998) Nickel biochemistry. Curr. Opin. Chem. Biol. **2:** 208–215
2 Ragsdale S. W. and Kumar M. (1996) Nickel-containing carbon monoxide dehydrogenase/acetyl-CoA synthase. Chem. Rev. **96:** 2515–2540
3 Maroney M. J. (1999) Structure/function relationships in nickel metallobiochemistry. Curr. Opin. Chem. Biol. **3:** 188–199
4 Ermler U., Grabarse W., Shima S., Goubeaud M. and Thauer R. K. (1998) Active sites of transition-metal enzymes with a focus on nickel. Curr. Opin. Struct. Biol. **8:** 749–758
5 Hausinger R. P. (1997) Metallocenter assembly in nickel-containing enzymes. J. Biol. Inorg. Chem. **2:** 279–286
6 Garcin E., Montet Y., Volbeda A., Hatchikian C., Frey M. and Fontecilla-Camps J. C. (1998) Structural bases for the catalytic mechanism of [NiFe] hydrogenases. Biochem. Soc. Trans. **26:** 396–401
7 Fontecilla-Camps J. C., Frey M., Garcin E., Hatchikian C., Montet Y., Piras C. et al. (1997) Hydrogenase: A hydrogen-metabolizing enzyme. What do the crystal structures tell us about its mode of action? Biochimie **79:** 661–666
8 Sumner J. B. (1926) The isolation and crystallization of the enzyme urease. J. Biol. Chem **69:** 435–441
9 Dixon N. E., Gazzola C., Blakeley R. L. and Zerner B. (1975) Jack Bean urease (EC 3.5.1.5). A metalloenzyme. A simple biological role for nickel? J. Am. Chem. Soc. **97:** 4131–4133
10 Mobley H. L. T. and Hausinger R. P. (1989) Microbial urease: significance, regulation and molecular characterization. Microbiol. Rev. **53:** 85–108
11 Benini S., Rupniewski W. R., Wilson K. S., Miletti S., Ciurli S. and Mangani S. (1999) A new proposal for urease mechanism based on the crystal structures of the native and inhibited enzyme from *Bacillus pasteurii*: why urea hydrolysis costs two nickels. Structure **7:** 205–216
12 Griffith D. P., Musher D. M. and Hin C. (1976) The primary cause of infection-induced urinary stones. Invest. Urol. **13:** 346–350
13 Braude A. I. and Siemienski J. (1960) Role of bacterial urease in experimental pyelonephritis. J. Bacteriol. **80:** 171–179
14 Mobley H. L. and Warren J. W. (1987) Urease-positive bacteria and obstruction of long-term urinary catheters. J. Clin. Microbiol. **25:** 2216–2217
15 Pérez-Pérez G. I., Olivares A. Z., Cover T. L. and Blaser M. J. (1992) Characteristics of *Helicobacter pylori* variants selected for urease deficiency. Infect. Immun. **60:** 3658–3663
16 Segal E. D., Shon J. and Tompkins L. S. (1992) Characterization of *Helicobacter pylori* urease mutants. Infect. Immun. **60:** 1883–1889
17 Jabri E., Carr M. B., Hausinger R. P. and Karplus P. A. (1995) The crystal structure of urease from *Klebsiella aerogenes*. Science **268:** 998–1004
18 Hausinger R. P. (1993) Urease. In: The Biochemistry of Nickel, p. 23–57, Plenum Press, New York
19 Jabri E. and Karplus P. A. (1996) Structures of the *Klebsiella aerogenes* urease apoenzyme and two active-site mutants. Biochemistry **35:** 10616–10626
20 Benini S., Rupniewski W. R., Wilson K. S., Ciurli S. and Mangani S. (1998) The complex of *Bacillus pasteurii* urease with b-mercaptoethanol from X-ray data at 1.65 Å resolution. J. Biol. Inorg. Chem. **3:** 268–273
21 Pearson M. A., Schaller R. A., Michel L. O., Karplus P. A. and Hausinger R. P. (1998) Chemical rescue of *Klebsiella aerogenes* urease variants lacking the carbamylated-lysine nickel ligand. Biochemistry **37:** 6214–6220
22 Pearson M. A., Michel L. O., Hausinger R. P. and Karplus P. A. (1997) Structures of Cys319 variants and acetohydroxamate-inhibited *Klebsiella aerogenes* urease. Biochemistry **36:** 8164–8172
23 Wang S., Lee M. H., Hausinger R. P., Clark P. A., Wilcox D. E. and Scott R. A. (1994) Structure of the dinuclear active site of urease. X-ray absorption spectroscopic study of native and 2-mercaptoethanol-inhibited bacterial and plant enzymes. Inorg. Chem. **33:** 1589–1593
24 Karplus P. A., Pearson M. A. and Hausinger R. P. (1997) 70 years of crystalline urease: what have we learned? Acc. Chem. Res. **30:** 330–337
25 Adams M. W. W. (1990) The structure and mechanism of iron-hydrogenases. Biochim. Biophys. Acta **1020:** 115–145
26 Li C., Peck H. D. Jr, LeGall J. and Przybyla A. E. (1987) Cloning, characterization and sequencing of the genes encoding the large and small subunits of the periplasmic [NiFe] hydrogenase of *Desulfovibrio gigas*. DNA **6:** 539–551
27 Voordouw G., Menon N. K., LeGall J., Choi E. S., Peck H. D. Jr and Przybyla A. E. (1989) Analysis and comparison of nucleotide sequences encoding the genes for [NiFe] and [NiFeSe] hydrogenases from *Desulfovibrio gigas* and *Desulfovibrio baculatus*. J. Bacteriol. **171:** 2894–2899
28 Zirngibl C., van Dongen W., Schwörer B., von Bünau R., Richter M., Klein A. et al. (1992) H_2-forming methylenetetrahydromethanopterin dehydrogenase, a novel type of hydrogenase without iron-sulfur clusters in methanogenic *archaea*. Eur. J. Biochem **208:** 511–520
29 Kovacs K. L., Seefeldt L. C., Tigyi G., Doyle C. M., Mortenson L. E. and Arp D. J. (1989) Immunological relationships among hydrogenases. J. Bacteriol. **171:** 430–435
30 Sayavedra-Soto L. A. and Arp D. J. (1993) In *Azotobacter vinelandii* hydrogenase, substitution of serine for the cysteine residues at positions 62, 65, 289, 292 in the small (HoxK) subunit affects H_2 oxidation. J. Bacteriol. **175:** 3414–3421
31 Ballantine S. P. and Boxer D. H. (1986) Isolation and characterisation of a soluble active fragment of hydrogenase isoenzyme 2 from the membranes of anaerobically grown *Escherichia coli*. Eur. J. Biochem. **156:** 277–284
32 Przybyla A. E., Robbins J., Menon N. and Peck H. D. Jr (1992) Structure-function relationships among the nickel-containing hydrogenases. FEMS Microbiol. Rev. **8:** 109–135
33 He S. H., Teixeira M., LeGall J., Patil D. S., Moura I., Moura J. J. et al. (1989) EPR studies with ^{77}Se-enriched (NiFeSe) hydrogenase of *Desulfovibrio baculatus*. Evidence for a selenium ligand to the active site nickel. J. Biol. Chem. **264:** 2678–2682
34 Eidsness M. K., Scott R. A., Prickril B. C., DerVartanian D. V., Legall J., Moura I. et al. (1989) Evidence for selenocysteine coordination to the active site nickel in the [NiFeSe] hydrogenases from *Desulfovibrio baculatus*. Proc. Natl. Acad. Sci. USA **86:** 147–151
35 Volbeda A., Charon M.-H., Piras C., Hatchikian E. C., Frey M. and Fontecilla-Camps J. C. (1995) Crystal structure of the nickel-iron hydrogenase from *Desulfovibrio gigas*. Nature **373:** 580–587
36 Volbeda A., Garcin E., Piras C., de Lacey A. L., Fernandez V. M., Hatchikian E. C. et al. (1996) Structure of the [NiFe] hydrogenase active site: evidence for biologically uncommon Fe ligands. J. Am. Chem. Soc. **118:** 12989–12996
37 Higuchi Y., Yagi T. and Yasuoka N. (1997) Unusual ligand structure in Ni-Fe active center and an additional Mg site

in hydrogenase revealed by high resolution X-ray structure analysis. Structure **5:** 1671–1680
38 Higuchi Y., Ogata H., Miki K., Yasuoka N. and Yagi T. (1999) Removal of the bridging ligand atom at the Ni-Fe active site of [NiFe] hydrogenase upon reduction with H_2, as revealed by X-ray structure analysis at 1.4 Å resolution. Structure **7:** 549–556
39 Maier T., Jacobi A., Sauter M. and Böck A. (1993) The product of the *hypB* gene, which is required for nickel incorporation into hydrogenases, is a novel guanine nucleotide-binding protein. J. Bacteriol. **175:** 630–635
40 Maier T., Lottspeich F. and Böck A. (1995) GTP hydrolysis by HypB is essential for nickel insertion into hydrogenases of *Escherichia coli*. Eur. J. Biochem. **230:** 133–138
41 Bagley K. A., Garderen C. J. V., Chen M., Duin E. C., Albracht S. P. J. and Woodruff W. H. (1994) Infrared studies on the interaction of carbon monoxide with divalent nickel in hydrogenase from *Chromatium vinosum*. Biochemistry **33:** 9229–9236
42 Bagley K. A., Duin E. C., Roseboom W., Albracht S. P. J. and Woodruff W. H. (1995) Infrared-detectable groups sense changes in charge density on the nickel center in hydrogenase from *Chromatium vinosum*. Biochemistry **34:** 5527–5535
43 Happe R. P., Roseboom W., Pierik A. J., Albracht S. P. J. and Bagley K. A. (1997) Biological activation of hydrogen. Nature **385:** 126
44 Pierik A. J., Roseboom W., Happe R. P., Bagley K. A. and Albracht S. P. J. (1999) Carbon monoxide and cyanide as intrinsic ligands to iron in the active site of [NiFe]-hydrogenases. J. Biol. Chem. **274:** 3331–3337
45 Van Der Spek T. M., Arendsen A. F., Happe R. P., Yun S., Bagley K. A., Stufkens D. J. et al. (1996) Similarities in the architecture of the active sites of Ni-hydrogenases and Fe-hydrogenases detected by means of infrared spectroscopy. Eur. J. Biochem. **237:** 629–634
46 Pierik A. J., Hulstein M., Hagen W. R. and Albracht S. P. (1998) A low-spin iron with CN and CO as intrinsic ligands forms the core of the active site in [Fe]-hydrogenases. Eur. J. Biochem. **258:** 572–578
47 Surerus K. K., Chen M., van der Zwaan J. W., Rusnak F. M., Kolk M., Duin E. C. et al. (1994) Further characterization of the spin coupling observed in oxidized hydrogenase from *Chromatium vinosum*. A Mössbauer and multifrequency EPR study. Biochemistry **33:** 4980–4993
48 Hirsch P. (1968) Photosynthetic bacterium growing under carbon monoxide. Nature **217:** 555–556
49 Uffen R. L. (1976) Anaerobic growth of a *Rhodopseudomonas* species in the dark with carbon monoxide as sole carbon and energy substrate. Proc. Natl. Acad. Sci. USA **73:** 3298–3302
50 Uffen R. L. (1981) Metabolism of carbon monoxide. Enzyme Microb. Technol. **3:** 197–206
51 Uffen R. L. (1983) Metabolism of carbon monoxide by *Rhodopseudomonas gelatinosa*: cell growth and properties of the oxidation system. J. Bacteriol. **155:** 956–965
52 Bonam D., Murrell S. A. and Ludden P. W. (1984) Carbon monoxide dehydrogenase from *Rhodospirillum rubrum*. J. Bacteriol. **159:** 693–699
53 Bonam D. and Ludden P. W. (1987) Purification and characterization of carbon monoxide dehydrogenase, a nickel, zinc, iron-sulfur protein, from *Rhodospirillum rubrum*. J. Biol. Chem. **262:** 2980–2987
54 Bonam D., McKenna M. C., Stephens P. J. and Ludden P. W. (1988) Nickel-deficient carbon monoxide dehydrogenase from *Rhodospirillum rubrum*: *In vivo* and *in vitro* activation by exogenous nickel. Proc. Natl. Acad. Sci. USA **85:** 31–35
55 Ensign S. A., Campbell M. J. and Ludden P. W. (1990) Activation of the nickel-deficient carbon monoxide dehydrogenase from *Rhodospirillum rubrum*: kinetic characterization and reductant requirement. Biochemistry **29:** 2162–2168
56 Ensign S. A., Bonam D. and Ludden P. W. (1989) Nickel is required for the transfer of electrons from carbon monoxide to the iron-sulfur centers of carbon monoxide dehydrogenase from *Rhodospirillum rubrum*. Biochemistry **28:** 4968–4973
57 Spangler N. J., Meyers M. R., Gierke K. L., Kerby R. L., Roberts G. P. and Ludden P. W. (1998) Substitution of valine for histidine 265 in carbon monoxide dehydrogenase from *Rhodospirillum rubrum* affects activity and spectroscopic states. J. Biol. Chem. **273:** 4059–4064
58 Ensign S. A., Hyman M. R. and Ludden P. W. (1989) Nickel specific, slow-binding, inhibition of carbon monoxide dehydrogenase from *Rhodospirillum rubrum* by cyanide. Biochemistry **28:** 4973–4979
59 Smith E. T., Ensign S. A., Ludden P. W. and Feinberg B. A. (1992) Direct electrochemical studies of hydrogenase and CO dehydrogenase. Biochem. J. **285:** 181–185
60 Spangler N. S., Lindahl P. A., Bandarian V. and Ludden P. W. (1996) Spectroelectrochemical characterization of the metal centers in carbon monoxide dehydrogenase (CODH) and nickel-deficient CODH from *Rhodospirillum rubrum*. J. Biol. Chem. **271:** 7973–7977
61 Stephens P. J., McKenna M.-C., Ensign S. A., Bonam D. and Ludden P. W. (1989) Identification of a Ni- and Fe-containing cluster in *Rhodospirillum rubrum* carbon monoxide dehydrogenase. J. Biol. Chem. **264:** 16347–16350
62 Hu Z., Spangler N. J., Anderson M. E., Xia J., Ludden P. W., Lindahl P. A. et al. (1996) Nature of the C-cluster in Ni-containing carbon monoxide dehydrogenases. J. Am. Chem. Soc. **118:** 830–845
63 Tan G. O., Ensign S. A., Ciurli S., Scott M. J., Hedman B., Holm R. H. et al. (1992) On the structure of the nickel/iron/sulfur center of the carbon monoxide dehydrogenase from *Rhodospirillum rubrum*: an X-ray absorption spectroscopy study. Proc. Natl. Acad. Sci. USA **89:** 4427–4431
64 Hausinger R. P. (1993) Carbon monoxide dehydrogenase. In: The Biochemistry of Nickel, pp. 107–145, Plenum Press, New York
65 Kumar M., Lu W.-P., Liu L. and Ragsdale S. W. (1993) Kinetic evidence that carbon monoxide dehydrogenase catalyzes the oxidation of carbon monoxide and the synthesis of acetyl-CoA at separate metal centers. J. Am. Chem. Soc. **115:** 11646–11647
66 Hu S.-I., Drak H. L. and Wood H. G. (1982) Synthesis of acetyl coenzyme A from carbon monoxide, methyltetrahydrofolate, and coenzyme A by enzymes from *Clostridium thermoaceticum*. J. Bacteriol. **149:** 440–448
67 Ragsdale S. W. (1991) Enzymology of the acetyl-CoA pathway of CO_2 fixation. Crit. Rev. Biochem. Mol. Biol. **26:** 261–300
68 Wood H. G. and Ljungdahl L. G. (1991) Autotrophic character of the acetogenic bacteria. In: Variations in Autotrophic Life, pp. 201–250, Academic Press, New York
69 Ragsdale S. W., Ljungdahl L. G. and DerVartanian D. V. (1983) Isolation of carbon monoxide dehydrogenase from *Acetobacterium woodii* and comparison of its properties with those of the *Clostridium thermoaceticum* enzyme. J. Bacteriol. **155:** 1224–1237
70 Ragsdale S. W., Clark J. E., Ljungdahl L. G., Lundie L. L. and Drake H. L. (1982) Properties of purified carbon monoxide dehydrogenase from *Clostridium thermoaceticum*, a nickel, iron-sulfur protein. J. Biol. Chem. **258:** 2364–2369
71 Xia J. Q., Sinclair J. F., Baldwin T. O. and Lindahl P. A. (1996) Carbon monoxide dehydrogenase from *Clostridium thermoaceticum*: quaternary structure, stoichiometry of its SDS-induced dissociation and characterization of the faster-migrating form. Biochemistry **35:** 1965–1971
72 Shin W. and Lindahl P. A. (1992) Discovery of a labile nickel ion required for CO/acetyl-CoA exchange activity in the NiFe complex of carbon monoxide dehydrogenase from *Clostridium thermoaceticum*. J. Am. Chem. Soc. **114:** 9718–9719

73 Shin W. and Lindahl P. A. (1992) Function and CO binding properties of the NiFe complex in carbon monoxide dehydrogenase from *Clostridium thermoaceticum*. Biochemistry **31:** 12870–12875
74 Ferry J. G. (1992) Biochemistry of methanogenesis. Crit. Rev. Biochem. Mol. Biol. **27:** 473–503
75 Ferry J. G. (1995) CO-dehydrogenase. In: Ann. Rev. Microbiol., pp. 305–355, Ornston L. N., Balows A. and Greenberg E. P. (eds), Annual Reviews, Palo Alto, CA
76 Jetten M. S. M., Stams A. J. M. and Zehnder A. J. B. (1989) Isolation and characterization of acetyl-coenzyme A synthetase from *Methanothrix soehngenii*. J. Bacteriol. **171:** 5430–5435
77 Aceti D. J. and Ferry J. G. (1988) Purification and characterization of acetate kinase from acetate-grown *Methanosarcina thermophila*. Evidence for regulation of synthesis. J. Biol. Chem. **263:** 15444–15448
78 Lundie L. L. Jr and Ferry J. G. (1989) Activation of acetate by *Methanosarcina thermophila*. Purification and characterization of phosphotransacetylase. J. Biol. Chem. **264:** 18392–18396
79 Raybuck S. A., Ramer S. E., Abbanat D. R., Peters J. W., Orme-Johnson W. H., Ferry J. G. et al. (1991) Demonstration of carbon-carbon bond cleavage of acetyl coenzyme A by using isotopic exchange catalyzed by the CO dehydrogenase complex from acetate-grown *Methanosarcina thermophila*. J. Bacteriol. **173:** 929–932
80 Jetten M. S. M., Hagen W. R., Pierik A. J., Stams A. J. M. and Zehnder A. J. B. (1991) Paramagnetic centers and actyl-coenzyme A/CO exchange activity of carbon monoxide dehydrogenase from *Methanothrix soehngenii*. Eur. J. Biochem. **195:** 385–391
81 Grahame D. A. (1991) Catalysis of acetyl-CoA cleavage and tetrahydrosarcinapterin methylation by a carbon monoxide dehydrogenase-corrinoid enzyme complex. J. Biol. Chem. **266:** 22227–22233
82 Xia J., Hu Z., Popescu C. V., Lindahl P. A. and Münck E. (1997) Mössbauer and EPR study of the Ni-activated alpha-subunit of carbon monoxide dehydrogenase from *Clostridium thermoaceticum*. J. Am. Chem. Soc. **119:** 8301–8312
83 Hausinger R. P. (1993) Methyl Coenzyme M reductase. In: Biochemistry of Nickel, pp. 147–180, Plenum Press, New York
84 Thauer R. K. (1998) Biochemistry of methanogenesis: a tribute to Marjory Stephenson. Microbiology **144:** 2377–2406
85 Hedderich R. and Thauer R. K. (1988) *Methanobacterium thermoautotrophicum* contains a soluble enzyme system that specifically catalyzes the reduction of coenzyme M and 7-mercaptoheptanoylthreonine phosphate with H_2. FEBS Lett. **234:** 223–227
86 Hedderich R., Berkessel A. and Thauer R. K. (1990) Purification and properties of heterodisulfide reductase from *Methanobacterium thermoautotrophicum* (strain Marburg). Eur. J. Biochem. **193:** 255–261
87 Deppenmeier U., Blaut M., Mahlmann A. and Gottschalk G. (1990) Reduced coenzyme F_{420}-heterodisulfide oxidoreductase, a proton-translocating redox system in methanogenic bacteria. Proc. Natl. Acad. Sci. USA **87:** 9449–9453
88 Rospert S., Linder D., Ellermann J. and Thauer R. K. (1990) Two genetically distinct methyl-coenzyme M reductases in *Methanobacterium thermoautotrophicum* strain Marburg and delta H. Eur. J. Biochem. **194:** 871–877
89 Brenner M. C., Ma L., Johnso M. K. and Scott R. A. (1992) Spectroscopic characterization of the alternate form of S-methylcoenzyme M reductase from *Methanobacterium thermoautotrophicum* (strain delta H). Biochim. Biophys. Acta **1120:** 160–166
90 Bonacker L. G., Baudner S. and Thauer R. K. (1992) Differential expression of the two methyl-coenzyme M reductases in *Methanobacterium thermoautotrophicum* as determined immunochemically via isoenzyme-specific antisera [published erratum appears in Eur. J. Biochem. **207:** 1129]. Eur. J. Biochem. **206:** 87–92
91 Bonacker L. G., Baudner S., Morschel E., Bocher R. and Thauer R. K. (1993) Properties of the two isoenzymes of methyl-coenzyme M reductase in *Methanobacterium thermoautotrophicum*. Eur. J. Biochem. **217:** 587–595
92 Telser J. (1998) Structure and Bonding **91:** 32–63
93 Ermler U., Grabarse W., Shima S., Goubeaud M. and Thauer R. K. (1997) Crystal structure of methyl-coenzyme M reductase: the key enzyme of biological methane formation. Science **278:** 1457–1462
94 Goubeaud M., Schreiner G. and Thauer R. K. (1997) Purified methyl-coenzyme-M reductase is activated when the enzyme-bound coenzyme F_{430} is reduced to the nickel(I) oxidation state by titanium(III) citrate. Eur. J. Biochem. **243:** 110–114
95 Youn H. D., Kim E. J., Roe J. H., Hah Y. C. and Kang S. O. (1996) A novel nickel-containing superoxide dismutase from *Streptomyces* spp. Biochem. J. **318:** 889–896
96 Kim F. J., Kim H. P., Hah Y. C. and Roe J. H. (1996) Differential expression of superoxide dismutases containing Ni and Fe/Zn in *Streptomyces coelicolor*. Eur. J. Biochem. **241:** 178–185
97 Kim E. J., Chung H. J., Suh B., Hah Y. C. and Roe J. H. (1998) Transcriptional and post-transcriptional regulation by nickel of *sodN* gene encoding nickel-containing superoxide dismutase from *Streptomyces coelicolor Muller*. Mol. Microbiol. **27:** 187–195
98 Clugston S. L., Barnard J. F., Kinach R., Miedema D., Ruman R., Daub E. et al. (1998) Overproduction and characterization of a dimeric non-zinc glyoxalase I from *Escherichia coli*: evidence for optimal activation by nickel ions. Biochemistry **37:** 8754–8763
98a Wulfing C., Lombardero J. and Pluckthun A. (1994) An *Escherichia coli* protein consisting of a domain homologous to FK506-binding proteins (FKBP) and a new metal-binding motif. J. Biol. Chem. **269:** 2895–2901
99 Abelson P. H. and Aldous E. (1950) Ion antagonisms in microorganisms: interference of normal magnesium metabolism by nickel, cobalt, cadmium, zinc and manganese. J. Bacteriol. **60:** 401–413
100 Webb M. (1970) Interrelationships between the utilization of magnesium and the uptake of other bivalent cations by bacteria. Biochim. Biophys. Acta **222:** 428–439
101 Webb M. (1970) The mechanism of acquired resistance to Co^{2+} and Ni^{2+} in gram-positive and gram-negative bacteria. Biochim. Biophys. Acta **222:** 440–446
102 Park M. H., Wong B. B. and Lusk J. E. (1976) Mutants in three genes affecting transport of magnesium in *Escherichia coli*: genetics and physiology. J. Bacteriol. **126:** 1096–1103
103 Roof S. K. and Maguire M. E. (1994) Magnesium transport systems: genetics and protein structure. J. Am. Coll. Nutr. **13:** 424–428
104 Snavely M. D., Florer J. B., Miller C. G. and Maguire M. E. (1989) Magnesium transport in Salmonella typhimurium: $^{28}Mg^{2+}$ transport by the CorA, MgtA, and MgtB systems. J. Bacteriol. **171:** 4761–4766
105 Snavely M. D., Gravina S. A., Cheung T. T., Miller C. G. and Maguire M. E. (1991) Magnesium transport in *Salmonella typhimurium*. Regulation of *mgtA* and *mgtB* expression. J. Biol. Chem. **266:** 824–829
106 Hmiel S. P., Snavely M. D., Miller C. G. and Maguire M. E. (1986) Magnesium transport in *Salmonella typhimurium*: characterization of magnesium influx and cloning of a transport gene. J. Bacteriol. **168:** 1444–1450
107 Smith R. L., Banks J. L., Snavely M. D. and Maguire M. E. (1993) Sequence and topology of the CorA magnesium transport systems of *Salmonella typhimurium* and *Escherichia coli*. Identification of a new class of transport protein. J. Biol. Chem. **268:** 14071–14080
108 Smith R. L. and Maguire M. E. (1995) Distribution of the CorA Mg^{2+} transport system in gram-negative bacteria. J. Bacteriol. **177:** 1638–1640

109 Tao T., Snavely M. D., Farr S. G. and Maguire M. E. (1995) Magnesium transport in *Salmonella typhimurium*: mgtA encodes a P-type ATPase and is regulated by Mg^{2+} in a manner similar to that of the *mgtB* P-type ATPase. J. Bacteriol. **177:** 2654–2662

110 Smith D. L., Tao T. and Maguire M. E. (1993) Membrane topology of a P-type ATPase. The MgtB magnesium transport protein of *Salmonella typhimurium*. J. Biol. Chem. **268:** 22469–22479

111 Snavely M. D., Florer J. B., Miller C. G. and Maguire M. E. (1989) Magnesium transport in Salmonella typhimurium: expression of cloned genes for three distinct Mg^{2+} transport systems. J. Bacteriol. **171:** 4752–4760

112 Smith R. L., Thompson L. J. and Maguire M. E. (1995) Cloning and characterization of MgtE, a putative new class of Mg^{2+} transporter from *Bacillus firmus* OF4. J. Bacteriol. **177:** 1233–1238

113 Eitinger T. and Friedrich B. (1997) Microbial nickel transport and incorporation into hydrogenases. In: Transition Metals in Microbial Metabolism, pp. 235–256, Winkelmann G. and Carrano C. J. (eds), Harwood Academic Publishers, London

114 Lundie L.L. Jr, Yang H. C., Heinonen J. K., Dean S. I. and Drake H. L. (1988) Energy-dependent, high-affinity transport of nickel by the acetogen *Clostridium thermoaceticum*. J. Bacteriol. **170:** 5705–5708

115 Bryson M. F. and Drake H. L. (1988) Energy-dependent transport of nickel by *Clostridium pasteurianum*. J. Bacteriol. **170:** 234–238

116 Campbell P. M. and Smith G. D. (1986) Transport and accumulation of nickel ions in the cyanobacterium *Anabaena cylindrica*. Arch. Biochem. Biophys. **244:** 470–477

117 Partridge C. D. and Yates M. G. (1982) Effect of chelating agents on hydrogenase in *Azotobacter chroococcum*. Evidence that nickel is required for hydrogenase synthesis. Biochem. J. **204:** 339–344

118 Baudet C., Sprott G. D. and Patel G. B. (1988) Adsorption and uptake of nickel in *Methanothrix concilii*. Arch. Microbiol. **150:** 338–342

119 Jarrell K. F. and Sprott G. D. (1982) Nickel transport in *Methanobacterium bryantii*. J. Bacteriol. **151:** 1195–1203

120 Stults L. W., Mallick S. and Maier R. J. (1987) Nickel uptake in *Bradyrhizobium japonicum*. J. Bacteriol. **169:** 1398–1402

121 Eitinger T. and Friedrich B. (1991) Cloning, nucleotide sequence, and heterologous expression of a high-affinity nickel transport gene from *Alcaligenes eutrophus*. J. Biol. Chem. **266:** 3222–3227

122 Wolfram L., Friedrich B. and Eitinger T. (1995) The *Alcaligenes eutrophus* protein HoxN mediates nickel transport in *Escherichia coli*. J. Bacteriol. **177:** 1840–1843

123 Eitinger T., Wolfram L., Degen O. and Anthon C. (1997) A Ni^{2+} binding motif is the basis of high affinity transport of the Alcaligenes eutrophus nickel permease. J. Biol. Chem. **272:** 17139–17144

124 Fu C., Javedan S., Moshiri F. and Maier R. J. (1994) Bacterial genes involved in incorporation of nickel into a hydrogenase enzyme. Proc. Natl. Acad. Sci. USA **91:** 5099–5103

125 Maeda M., Hidaka M., Nakamura A., Masaki H. and Ouzumi T. (1994) Cloning, sequencing, and expression of thermophilic *Bacillus* sp. strain TP-90 urease complex in *Escherichia coli*. J. Bacteriol. **176:** 432–442

126 Mobley H. L., Garner R. M. and Bauerfeind P. (1995) *Helicobacter pylori* nickel-transport gene *nixA*: synthesis of catalytically active urease in *Escherichia coli* independent of growth conditions. Mol. Microbiol. **16:** 97–109

127 Fulkerson J. F. Jr, Garner R. M. and Mobley H. L. (1998) Conserved residues and motifs in the NixA protein of *Helicobacter pylori* are critical for the high affinity transport of nickel ions. J. Biol. Chem. **273:** 235–241

128 Hidalgo E., Palacios J. M., Murillo J. and Ruiz-Argueso T. (1992) Nucleotide sequence and characterization of four additional genes of the hydrogenase structural operon from *Rhizobium leguminosarum bv. viciae*. J. Bacteriol. **174:** 4130–4139

129 McMillan D. J., Mau M. and Walker M. J. (1998) Characterisation of the urease gene cluster in *Bordetella bronchiseptica*. Gene **208:** 243–251

130 Hendricks J. K. and Mobley H. L. (1997) *Helicobacter pylori* ABC transporter: effect of allelic exchange mutagenesis on urease activity. J. Bacteriol. **179:** 5892–5902

131 Navarro C., Wu L. F. and Mandrand-Berthelot M. A. (1993) The *nik* operon of *Escherichia coli* encodes a periplasmic binding-protein-dependent transport system for nickel. Mol. Microbiol. **9:** 1181–1191

132 De Pina K., Desjardin V., Mandrand-Berthelot M. A., Giordano G. and Wu L. F. (1999) Isolation and characterization of the *nikR* gene encoding a nickel-responsive regulator in *Escherichia coli*. J. Bacteriol. **181:** 670–674

133 Ames G. R.-L. (1986) Bacterial periplasmic transport systems: structure, mechanism, and evolution. Annu. Rev. Biochem. **55:** 397–426

134 de Pina K., Navarro C., McWalter L., Boxer D. H., Price N. C., Kelly S. M. et al. (1995) Purification and characterization of the periplasmic nickel-binding protein NikA of *Escherichia coli* K12. Eur. J. Biochem. **227:** 857–865

135 Komeda H., Kobayashi M. and Shimizu S. (1997) A novel transporter involved in cobalt uptake. Proc. Natl. Acad. Sci. USA **94:** 36–41

136 Bhattacharyya P. (1975) Active transport of manganese in isolated membrane vesicles of *Bacillus subtilis*. J. Bacteriol. **123:** 123–127

137 Jones B. D. and Mobley H. L. (1989) *Proteus mirabilis* urease: nucleotide sequence determination and comparison with jack bean urease. J. Bacteriol. **171:** 6414–6422

138 Island M. D. and Mobley H. L. (1995) *Proteus mirabilis* urease: operon fusion and linker insertion analysis of ure gene organization, regulation, and function. J. Bacteriol. **177:** 5653–5660

139 Moble H. L. (1996) The role of *Helicobacter pylori* urease in the pathogenesis of gastritis and peptic ulceration. Aliment. Pharmacol. Ther. **10:** 57–64

140 Cussac V., Ferrero R. L. and Labigne A. (1992) Expression of *Helicobacter pylori* urease genes in *Escherichia coli* grown under nitrogen-limiting conditions. J. Bacteriol. **174:** 2466–2473

141 Mulrooney S. B. and Hausinger R. P. (1990) Sequence of the *Klebsiella aerogenes* urease genes and evidence for accessory proteins facilitating nickel incorporation. J. Bacteriol. **172:** 5837–5843

142 Lee M. H., Mulrooney S. B., Renner M. J., Markowicz Y. and Hausinger R. P. (1992) *Klebsiella aerogenes* urease gene cluster: sequence of *ureD* and demonstration that four accessory genes (*ureD*, *ureE*, *ureF*, and *ureG*) are involved in nickel metallocenter biosynthesis. J. Bacteriol. **174:** 4324–4330

143 Moncrief M. B. C. and Hausinger R. P. (1996) Nickel incorporation into urease. In: Mechanisms of Metallocenter Assembly, Hausinger R. P., Eichhorn G. L. and Marzilli L. G. (eds) vol. 11, pp. 151–171, New York, VCH Publishers

144 Lee M. H., Mulrooney S. B. and Hausinger R. P. (1990) Purification, characterization, and in vivo reconstitution of *Klebsiella aerogenes* urease apoenzyme. J. Bacteriol. **172:** 4427–4431

145 Park I.-S., Carr M. B. and Hausinger R. P. (1994) In vitro activation of urease apoprotein and role of UreD as a chaperone required for nickel metallocenter assembly. Proc. Natl. Acad. Sci. USA **91:** 3233–3237

146 Park I.-S. and Hausinge R. P. (1995) Requirement of carbon dioxide for in vitro assembly of urease nickel metallocenter. Science **267:** 1156–1158

147 Park I.-S. and Hausinger R. P. (1996) Metal ion interaction with urease and UreD-urease apoproteins. Biochemistry **35:** 5345–5352

148 Sriwanthana B., Island M. D., Maneval D. and Mobley H. L. (1994) Single-step purification of *Proteus mirabilis* urease accessory protein UreE, a protein with a naturally occurring histidine tail, by nickel chelate affinity chromatography. J. Bacteriol. **176:** 6836–6841
149 Lee M. H., Pankratz H. S., Wang S., Scott R. A., Finnegan M. G., Johnson M. K. et al. (1993) Purification and characterization of *Klebsiella aerogenes* UreE protein: A nickel-binding protein that functions in urease metallocenter assembly. Protein Science **2:** 1042–1052
150 Brayman T. G. and Hausinger R. P. (1996) Purification, characterization and functional analysis of a truncated *Klebsiella aerogenes* UreE urease accessory protein lacking the histidine-rich carboxyl terminus. J. Bacteriol. **178:** 5410–5416
151 Colpas G. J., Brayman T. G., Ming L. and Hausinger R. P. (1999) Identification of metal-binding residues in the *Klebsiella aerogenes* urease nickel metallochaperone, UreD. Biochemistry **38:** 4078–4088
152 Park I. S. and Hausinger R. P. (1995) Evidence for the presence of urease apoprotein complexes containing UreD, UreF, and UreG in cells that are competent for in vivo enzyme activation. J. Bacteriol. **177:** 1947–1951
153 Moncrief M. B. and Hausinger R. P. (1996) Purification and activation properties of UreD-UreF-urease apoprotein complexes. J. Bacteriol. **178:** 5417–5421
154 Sriwanthana B., Island M. D. and Mobley H. L. (1993) Sequence of the *Proteus mirabilis* urease accessory gene *ureG*. Gene **129:** 103–106
155 Moncrief M. B. and Hausinger R. P. (1997) Characterization of UreG, identification of a UreD-UreF-UreG complex, and evidence suggesting that a nucleotide-binding site in UreG is required for in vivo metallocenter assembly of *Klebsiella aerogenes* urease. J. Bacteriol. **179:** 4081–4086
156 Jacobi A., Rossmann R. and Böck A. (1992) The *hyp* operon gene products are required for the maturation of catalytically active hydrogenase isoenzymes in *Escherichia coli*. Arch. Microbiol. **158:** 444–451
157 Lutz S., Jacobi A., Schlensog V., Bohm R., Sawers G. and Böck A. (1991) Molecular characterization of an operon (*hyp*) necessary for the activity of the three hydrogenase isoenzymes in *Escherichia coli*. Mol. Microbiol. **5:** 123–135
158 Waugh R. and Boxer D. H. (1986) Pleiotropic hydrogenase mutants of *Escherichia coli* K12: growth in the presence of nickel can restore hydrogenase activity. Biochimie **68:** 157–166
159 Maier T. and Böck A. (1996) Nickel incorporation into hydrogenases. In: Mechanisms of Metallocenter Assembly, Hausinger R. P., Eichhorn G. L. and Marzilli L. G. (eds), vol. 11, pp. 173–92, New York, VCH Publishers
160 Hausinger R. P. (1993) Hydrogenase. In: The Biochemistry of Nickel, pp. 59–105, Plenum Press, New York
161 Rossmann R., Sauter M., Lottspeich F. and Böck A. (1994) Maturation of the large subunit (HYCE) of *Escherichia coli* hydrogenase 3 requires nickel incorporation followed by C-terminal processing at Arg537. Eur. J. Biochem. **220:** 377–384
162 Rey L., Imperial J., Palacios J.M. and Ruiz-Argüeso T. (1994) Purification of *Rhizobium leguminosarum* Hyp B, a nickel-binding protein required for hydrogenase synthesis. J. Bacteriol. **176:** 6066–6073
163 Fu C., Olson J. W. and Maier R. J. (1995) HypB protein of *Bradyrhizobium japonicum* is a metal-binding GTPase capable of binding 18 divalent nickel ions per dimer. Proc. Natl. Acad. Sci. USA **92:** 2333–2337
164 Colbeau A., Elsen L., Tomiyama M., Zorin N. A., Dimon B. and Vignais P. M. (1998) *Rhodobacter capsulatus* HypF is involved in regulation of hydrogenase synthesis through the HypUV proteins. Eur. J. Biochem. **251:** 65–71
165 Maier T., Binder U. and Böck A. (1996) Analysis of the *hydA* locus of *Escherichia coli*: two genes (*hydN* and *hypF*) involved in formate and hydrogen metabolism. Arch. Microbiol. **165:** 333–341
166 Drapal N. and Böck A. (1998) Interaction of the hydrogenase accessory protein HypC with HycE, the large subunit of *Escherichia coli* hydrogenase 3 during enzyme maturation. Biochemistry **37:** 2941–2948
167 Rey L., Fernandez D., Brito B., Hernando Y., Palacios J. M., Imperial J. et al. (1996) The hydrogenase gene cluster of *Rhizobium leguminosarum by viciae* contains an additional gene (*hypX*) which encodes a protein with sequence similarity to the N10-formyltetrahydrofolate-dependent enzyme family and is required for nickel-dependent hydrogenase processing and activity. Mol. Gen. Genet. **252:** 237–248
168 Maier T. and Böck A. (1996) Generation of active [NiFe] hydrogenase in vitro from a nickel-free precursor form. Biochemistry **35:** 10089–10093
169 Imperial J., Rey L., Palacios J. M. and Ruiz-Argueso T. (1993) HupK, a hydrogenase-ancillary protein from *Rhizobium leguminosarum*, shares structural motifs with the large subunit of NiFe hydrogenases and could be a scaffolding protein for hydrogenase metal cofactor assembly. Mol. Microbiol. **9:** 1305–1306
170 Allen R. M., Chatterjee R., Madden M. S., Ludden P. W. and Shah V. K. (1994) Biosynthesis of the iron-molybdenum cofactor of nitrogenase [published erratum appears in Crit Rev Biotechnol 1995 **15:** 104]. Crit. Rev. Biotechnol. **14:** 225–249
170a Vignais P. M., Dimon B., Zorin N. A., Colbeau A. and Elsen S. (1997) HupUV proteins of *Rhodobacter capsulatus* can bind H-2: Evidence from the H-D exchange reaction. J. Bacteriol. **179:** 290–292
170b Pierik A. J., Schmelz M., Lenz O., Friedrich B. and Albracht S. P. J. (1998) Characterization of the active site of a hydrogen sensor from *Alcaligenes eutrophus*. FEBS Lett. **438:** 231–235
171 Kerby R. L., Hong S. S., Ensign S. A., Coppoc L. J., Ludden P. W. and Roberts G. P. (1992) Genetic and physiological characterization of the *Rhodospirillum rubrum* carbon monoxide dehydrogenase system. J. Bacteriol. **174:** 5284–5294
172 Kerby R. L., Ludden P. W. and Roberts G. P. (1997) In vivo nickel insertion into the carbon monoxide dehydrogenase of *Rhodospirillum rubrum*: molecular and physiological characterization of *cooCTJ*. J. Bacteriol. **179:** 2259–2266
173 Fox J. D., He Y., Shelver D., Roberts G. P. and Ludden P. W. (1996) Characterization of the region encoding the CO-induced hydrogenase of *Rhodospirillum rubrum*. J. Bacteriol. **178:** 6200–6208
174 Shelver D., Kerby R. L., He Y. and Roberts G. P. (1995) Carbon monoxide-induced activation of gene expression in *Rhodospirillum rubrum* requires the product of *cooA*, a member of the cyclic AMP receptor protein family of transcriptional regulators. J. Bacteriol. **177:** 2157–2163
175 Shelver D., Kerby R. L., He Y. and Roberts G. P. (1997) CooA, a CO-sensing transcription factor from *Rhodospirillum rubrum*, is a CO-binding heme protein. Proc. Natl. Acad. Sci. USA **94:** 11216–11220
176 Aono S., Nakajima H., Saito K. and Okada M. (1996) A novel heme protein that acts as a carbon monoxide-dependent transcriptional activator in *Rhodospirillum rubrum*. Biochem. Biophys. Res. Comm. **228:** 752–756
177 He Y., Shelver D., Kerby R. L. and Roberts G. P. (1996) Characterization of a CO-responsive transcriptional activator from *Rhodospirillum rubrum*. J. Biol. Chem. **271:** 120–123
178 Kerby R. L., Ludden P. W. and Roberts G. P. (1995) Carbon monoxide-dependent growth of *Rhodospirillum rubrum*. J. Bacteriol. **177:** 2241–2244
179 Dernedde J., Eitinger T., Patenge N. and Friedrich B. (1996) *hyp* gene products in *Alcaligenes eutrophus* are part of a hydrogenase-maturation system. Eur. J. Biochem. **235:** 351–358
180 Watt R. K. and Ludden P. W. (1998) The identification, purification, and characterization of CooJ. J. Biol. Chem. **273:** 10019–10025

181 Maier R. J., Pihl T. D., Stults L. and Sray W. (1990) Nickel accumulation and storage in *Bradyrhizobium japonicum*. Appl. Environ. Microbiol. **56:** 1905–1911
182 Gonzalez H. and Jensen T. E. (1998) Nickel sequestering by polyphosphate bodies in *Staphylococcus aureus*. Microbios **93:** 179–185
183 Maupin-Furlow J. A. and Ferry J. G. (1996) Analysis of the CO dehydrogenase/acetyl-coenzyme A synthase operon of *Methanosarcina thermophila*. J. Bacteriol. **178:** 6849–6856
184 Bult C. J. et al. (1996) Complete genome sequence of the methanogenic archaeon, *Methanococcus jannaschii*. Science **273:** 1058–1073
185 Thauer R. K. and Bonacker L. G. (1994) Biosynthesis of coenzyme F_{430}, a nickel porphinoid involved in methanogenesis. In: The Biosynthesis of Tetrapyrrole Pigments, pp. 210–227, Chadwick D. J. and Ackrill K. (eds), Wiley, New York
186 Evans D. J. Jr, Evans D. G., Engstrand L. and Graham D. Y. (1992) Urease-associated heat shock protein of *Helicobacter pylori*. Infect. Immun. **60:** 2125–2127
187 Evans D. J. Jr, Evans D. G., Kirkpatrick S. S. and Graham D. Y. (1991) Characterization of the *Helicobacter pylori* urease and purification of its subunits. Microb. Pathog. **10:** 15–26
188 Suerbaum S., Thiberge J. M., Kansau I., Ferrero R. L. and Labigne A. (1994) *Helicobacter pylori hspA-hspB* heat-shock gene cluster: nucleotide sequence, expression, putative function and immunogenicity. Mol. Microbiol. **14:** 959–974
189 Kansau I., Guillain F., Thiberge J. M. and Labigne A. (1996) Nickel binding and immunological properties of the C-terminal domain of the *Helicobacter pylori* GroES homologue (HspA). Mol. Microbiol. **22:** 1013–1023
190 Kansau I. and Labigne A. (1996) Heat shock proteins of *Helicobacter pylori*. Aliment. Pharmacol. Ther. **10:** 51–56
191 Rodrigue A., Batia N., Muller M., Fayet O., Bohm R., Mandrand-Berthelot M. A. et al. (1996) Involvement of the GroE chaperonins in the nickel-dependent anaerobic biosynthesis of NiFe-hydrogenases of *Escherichia coli*. J. Bacteriol. **178:** 4453–4460
192 Ludden P. W., Roberts G. P., Kerby R. L., Spangler N., Fox J., Shelver D., et al. (1996) The biochemistry of CO dehydrogenase in *Rhodospirillum rubrum*. In: Microbial Growth on C_1 Compounds, pp. 183–190, Lidstrom M. E. and Tabita F. R. (eds), Kluwer Academic Publishers, Dordrecht